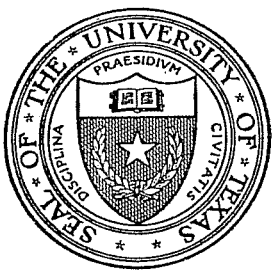

CESRL REPORT NO. 77-3
NOVEMBER 1977

STRENGTH OF HOOKED BAR ANCHORAGES IN BEAM-COLUMN JOINTS

By

ROBERT L. PINC
MICHAEL D. WATKINS
and
JAMES O. JIRSA

Report on a Research Project
Sponsored by
The Reinforced Concrete Research Council—Project 33

DEPARTMENT OF CIVIL ENGINEERING / Structures Research Laboratory
THE UNIVERSITY OF TEXAS, AUSTIN, TEXAS

STRENGTH OF HOOKED BAR ANCHORAGES IN BEAM-COLUMN JOINTS

by

Robert L. Pinc
Michael D. Watkins
and
James O. Jirsa

Report on a Research Project
Sponsored by
The Reinforced Concrete Research Council--Project 33

Civil Engineering Structures Research Laboratory
The University of Texas at Austin

November 1977

Author 1, Author
Author 2, Author
and
Author 3, Author

Report on a Research Project
Sponsored by
The Reinforced Concrete Research Council--Project 33

Civil Engineering Department
The University of Texas at Austin

August 19

SUMMARY OF REPORT

In order to investigate the influence of straight lead embedment and lightweight concrete on the strength of hooked bar anchorages, sixteen specimens were tested. These specimens and the method of testing were patterned after a previous study of hooked bar anchorages so that direct comparisons could be made. The specimens simulate typical beam-column joints. The lead embedment length varied with the depth of the column in which the bar was embedded. The bars were loaded in tension to failure to establish basic strength and stiffness characteristics. The slip of the anchored bars with respect to the concrete and stress transferred to the concrete along the bars were measured.

The results of the test program and the results of previous tests were combined to develop a relatively simple relationship between the embedded length of a hooked bar and strength. The advantage of the procedure is that the hook and the straight lead embedment are considered as a unit and the strength of the hooked bar anchorage is not coupled to development provisions for straight bars. Using the relationship developed for strength, the performance of the anchored bars appears to be within acceptable limits of serviceability as set by the ACI 318-71 Code.

C O N T E N T S

Chapter | Page

LIST OF TABLES

LIST OF FIGURES

NOTATION

A_b = area of bar, $in.^2$

C = factor for lightweight aggregate (ACI 318-71)

d_b = bar diameter, in.

f = bar stress, ksi

f'_c = concrete strength, psi

f_h = stress carried by standard hook, psi

f_ℓ = stress transferred along straight lead embedment, psi

f_u = measured ultimate stress, psi

f_y = yield strength of reinforcement, psi

ℓ' = minimum straight lead embedment, in.

ℓ_d = development length, in.

ℓ_{dh} = length of hooked bar anchorage, horizontal projection of hooked bar anchorage, in.

ℓ_ℓ = straight lead embedment, in.

ξ = constant for standard hook (ACI 318-71)

σ = standard deviation

ψ = factor reflecting confinement

Ω = constant for lightweight concrete

1. INTRODUCTION

1.1 Object and Scope

The object of this study was to examine the influence of lead embedment and lightweight aggregate concrete on the strength of hooked bar anchorages in beam-column joints. A total of 16 specimens was tested. The program was an extension of earlier work reported in Ref. 1. The specimens were full scale models of beam-column joints in order to eliminate scale effects and to permit the use of large diameter hooked bars which conform to ACI standards for hook geometry. The purpose of the study was to refine design recommendations made in Ref. 1 and 2.

1.2 Previous Work

In the studies reported by Marques and Jirsa [1], the tensile stress developed by a standard hook f_h was expressed by

$$f_h = 700(1 - 0.3d_b)\,\psi\sqrt{f'_c} \leq f_y \qquad (1.1)$$

where d_b is the diameter of the anchored bar and the value of ψ is varied according to the lateral confinement provided, varying between 1.0 and 1.8. If additional development length is required, the straight lead embedment length ℓ_ℓ between the initial section and the hook is calculated as follows:

$$\ell_\ell = [0.04A_b(f_y - f_h)/\sqrt{f'_c}\,] + \ell' \qquad (1.2)$$

where ℓ' is $4d_b$ or 4 in., whichever is greater.

While Eqs. 1.1 and 1.2 provided good agreement between measured and calculated hooked bar anchorage strengths, a number of shortcomings became evident. First, there were no data available for bars embedded in lightweight aggregate concrete. Second, the straight lead embedment

was a function of the development length equations for straight bars contained in ACI 318-71 [4]. Development length provisions are based on the results of tests in which stresses vary from a maximum at the lead end to zero at the tail end. For lead embedments ahead of a hook, the stress does not reduce to zero and the development length provisions do not necessarily extrapolate linearly with stress differentials. Additionally, very little data on variation of the length of straight lead embedments were available in the literature and in previous studies.

1.3 Acknowledgments

The work reported herein was part of an investigation supported by the Reinforced Concrete Research Council under Project 33. The program of investigation has been under the guidance of a Task Committee composed of the following persons:

D. J. Caldera, Chairman, TAMS, Engineers and Consultants, New York

J. F. McDermott, U. S. Steel Corporation, Monroeville, Pennsylvania

C. F. Corns, Headquarters, U. S. Air Force, Washington, D.C.

N. W. Hanson, Portland Cement Association, Skokie, Illinois

H. E. Nelson, City of Chicago, Illinois

P. F. Rice, Concrete Reinforcing Steel Institute, Chicago, Illinois

The project has been directed by J. O. Jirsa, Professor of Civil Engineering. Portions of the project formed parts of Master of Science theses submitted to The University of Texas at Austin by Mr. Robert L. Pinc and Mr. Michael D. Watkins. Special acknowledgment is due the Texas Aggregates and Concrete Association, which provided Mr. Watkins with partial support by awarding him the George C. Smith Memorial Scholarship.

The work was conducted in the Civil Engineering Structures Research Laboratory at the Balcones Research Center of The University of

Texas at Austin. Cadweld splices used in testing were donated by Erico Products, Inc., through the cooperation of Mr. James Barry. The lightweight aggregate materials were obtained through the Expanded Shale Clay and Slate Institute and were donated by the Material Service Corporation of Chicago. The help of Mr. Jim Fiala of Material Service Corporation is gratefully acknowledged.

2. TEST PROGRAM

2.1 Test Specimens

The test program was patterned after the hooked bar anchorage study conducted by Jirsa and Marques [1]. The same basic specimen configuration and testing procedure were used.

2.1.1 Specimen Geometry and Reinforcement. A typical exterior beam-column joint was simulated with the specimen shown in Fig. 2.1. The column cross section varied from 12 x 12 in. to 12 x 24 in. in increments of 3 in. All the specimens cast with lightweight aggregate concrete had column cross sections of 12 x 15 in. The assumed beam was 12 in. wide and 20 in. deep. The dimensions of the beam and column were chosen so that the specimen would be a realistic full-scale simulation of an exterior beam-column joint in typical concrete frame construction. The length of the column in all tests was 50 in. It was necessary to extend the column above and below the beam to eliminate lateral constraints in the joint region produced by the axial loading heads. It should be noted that the dimensions coincided with those used in the previous studies.

As seen in Fig. 2.1, the test specimen was cast without the beam extending from the joint. The anchored beam reinforcement was extended past the face of the column so that it could be loaded with hydraulic rams in the testing apparatus. The compression zone of the beam was simulated by a steel plate bearing against the face of the column over an area which approximated that of the compression zone of the assumed beam. This was considered to be a realistic model of forces on the joint after flexural cracking of the beam, with the exception that no provision was made to simulate the action of vertical beam shear on the joint. Beam shear, however, was not considered to have a significant influence on the anchorage behavior, as it is transferred to the column principally in the beam compression zone away from the hooked bar.

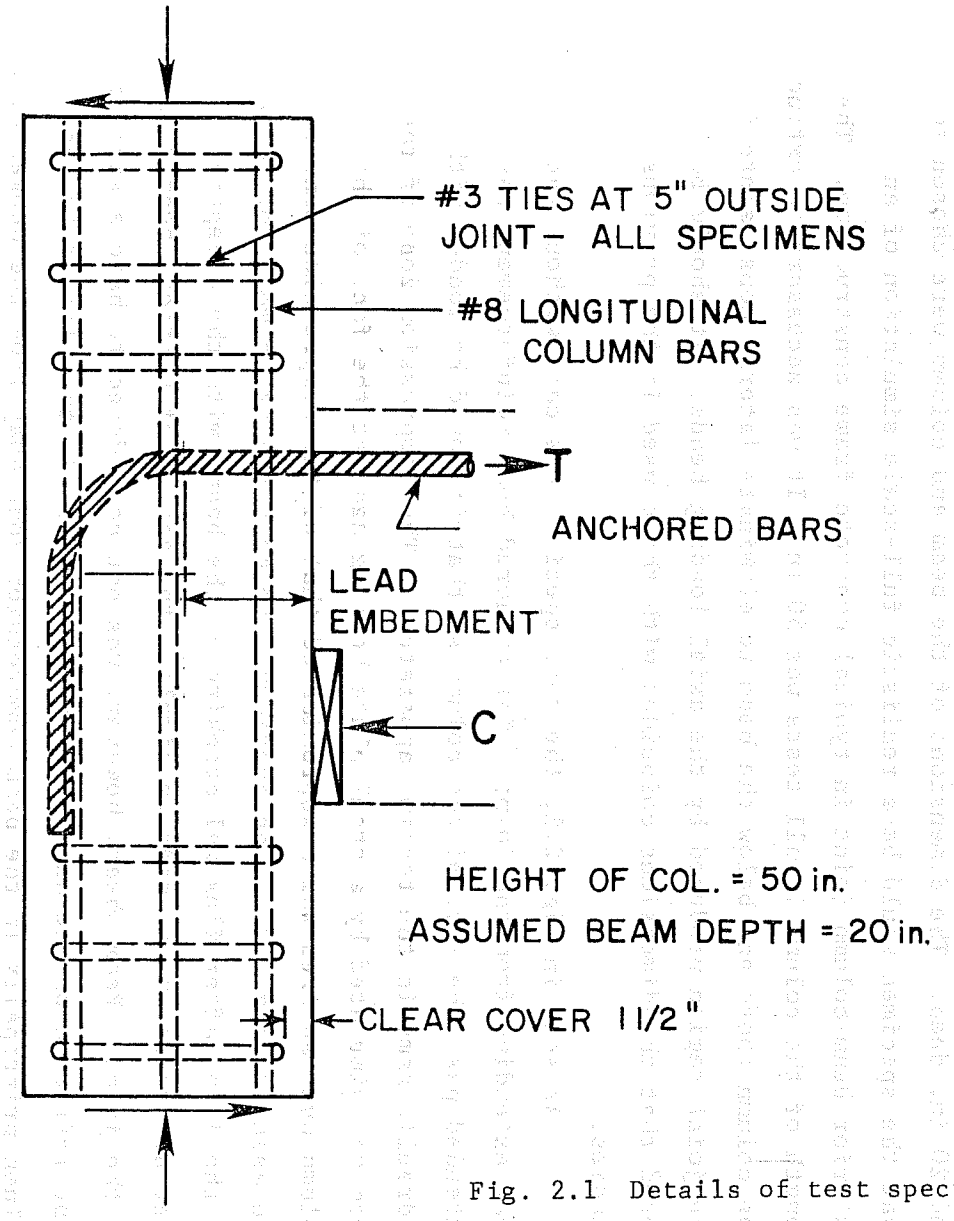

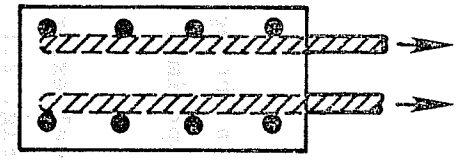

12 X 24 IN. COL.
12 X 21 IN. COL.

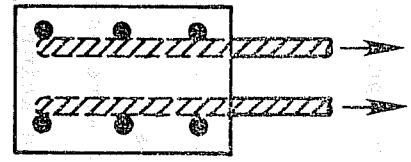

12 X 18 IN. COL.
12 X 15 IN. COL.

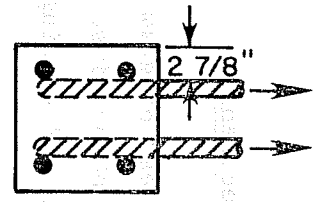

12 X 12 IN. COL.

Fig. 2.1 Details of test specimens

The 12 X 12 in. columns were reinforced with four #8 longitudinal column bars and #3 closed ties spaced at 5 in. c.c outside the joint. The 12 X 15 in. and 12 X 18 in. columns were reinforced with six #8 longitudinal column bars, while the 12 X 21 and 12 X 24 in. columns had eight #8 bars. Each of these specimens also was reinforced with #3 closed ties spaced at 5 in. c.c. outside the joint. The clear cover over the ties was 1-1/2 in. The anchored bars, the longitudinal bars, and the ties used throughout the study were Grade 60 steel. Yield for the #7 bars was 66 ksi, for the #9 bars was 65 ksi, and for the #11 bars was 57 to 60 ksi.

2.1.2 Variables. Table 2.1 summarizes the properties of the sixteen specimens tested in this study. The variables considered and the range of these variables are discussed below.

(a) Size of Anchored Bars. The embedment length tests were conducted with either #9 or #11 beam bars anchored in the columns. Previous tests, conducted with #7 and #11 bars, showed that the #7 bars almost reached their yield strength in the small 12 X 12 in. column and greatly exceeded it in the larger 12 X 15 column. In the case of specimens reaching well into the yield range, it is difficult to evaluate the influence of confinement and other variables if the concrete does not participate in the final failure. Therefore, to study the influence of embedment length on strength, it was felt that tests of #9 and #11 bars would provide more useful data. From a practical standpoint, bars larger than #11 would rarely be used in frame members. The series of tests with lightweight aggregate concrete was conducted using #7 and #11 beam bars. The use of #7 bars was warranted because it was felt that the splitting strength of the lightweight concrete was likely to be lower than normal weight concrete and failure would occur before the bars yielded.

(b) Lead Embedment Length. By varying the size of the column, the lead embedment before the hook portion of the anchored bar was varied. Values of lead embedment are tabulated in Table 2.1.

TABLE 2.1 PROPERTIES OF TEST SPECIMENS

Specimen	Bar Size	Lead Embedment in.	Column Size in.	Confinement		Column Load kips	Average Normal Stress psi	Concrete Strength ksi	Failure Type
				Cover in.	Ties in Joint				
Lead Embedment Series									
9-12	#9	4-3/8	12x12	2-7/8	None	108	750	4.7	Front pullout
9-15	#9	7-3/8	12x15	2-7/8	None	141	780	3.8	Side spalled
9-18	#9	10-3/8	12x18	2-7/8	None	181	800	4.7	Bar yielded
9-21	#9	13-3/8	12x21	2-7/8	None	202	800	3.6	Side spalled
11-15	#11	6	12x15	2-7/8	None	116	640	5.4	Side spalled
11-18	#11	9	12x18	2-7/8	None	173	800	4.7	Side spalled
11-21	#11	12	12x21	2-7/8	None	188	750	5.2	Bar yielded
11-24	#11	15	12x24	2-7/8	None	230	800	4.2	Bar yielded
Lightweight Aggregate Concrete Series									
11-90-1-L-AL	#11	6	12x15	2-7/8	None	154	850	4.2 (420)*	Side spalled
11-90-1-H-AL	#11	6	12x15	2-7/8	None	540	3000	4.8 (440)	Side spalled
11-90-1-L-AS	#11	6	12x15	2-7/8	None	154	850	5.6 (550)	Side spalled
11-90-1-L-FR	#11	6	12x15	2-7/8	None	154	850	4.7 (470)	Side spalled
11-180-1-L-FR	#11	6	12x15	2-7/8	None	154	850	4.8 (430)	Side spalled
11-90-3-L-FR	#11	6	12x15	2-7/8	#3 @ 5 in.	154	850	5.0 (410)	Side spalled
7-90-1-L-AS	#7	9-1/2	12x15	2-7/8	None	154	850	5.6 (540)	Bar yielded
7-90-1-L-FR	#7	9-1/2	12x15	2-7/8	None	154	850	4.5 (440)	Side spalled

*Split tensile concrete strength (p.si).

(c) Concrete. The concrete used in the lead embedment series was obtained commercially and specified to give approximately 4500 psi nominal compressive strength, which is the same compressive strength used in the previous study of hooked bar anchorage. The actual concrete strengths, however, varied from 3600 to 5400 psi. As will be discussed later, two specimens, 9-15 and 9-21 had concrete strengths of 3600 psi and 3800 psi with a poor quality aggregate.

Three basic mixes of lightweight concrete were used in the study. The mix proportions were computed on the basis of a 1 yd. batch and multiples of these proportions were used as needed. All three mixes were proportioned to give an average compressive strength f'_c of 4800 psi at 14 to 21 days. The lightweight aggregate used was "Materialite" lightweight aggregate, a coated expanded shale produced and supplied to this project by the Materialite plant located at Ottawa, Illinois. The coating is accomplished by fusing the outer surface of the aggregate into a sealed shell enclosing unconnected dead air cells. The coarse lightweight aggregate used was the Materialite medium gradation ranging from 3/8 in. to 3/16 in., and the lightweight fine aggregate used was the Materialite fine gradation ranging from 3/16 in. to 0 in. For the mixes that required normal weight fines, the local Colorado River sand fines were used.

The proportions for the lightweight concrete mixes were established on the basis of volumes in order to account for the differences in moisture content normally found in lightweight aggregates. Before each batch was mixed, the unit weight of coarse and fine lightweight aggregate was obtained and the mix was proportioned using the unit weights. Mix proportions for the three different mixes are given in Table 2.2. All three mixes had seven sacks of Type I portland cement and two and one-half ounces of an air entraining agent. Water was added as required to obtain a 6 in. slump. All specimens and control cylinders were stripped four to five days after casting and the curing was continued at room temperature until testing. The concrete strengths are listed for each specimen in Table 2.1, including split cylinder strengths.

TABLE 2.2 MIX PROPORTIONS FOR LIGHTWEIGHT CONCRETE (1 yd^3)

	All Lightweight (AL)	Fifty Percent Sand Replacement (FR)	All Sand (AS)
Cement, lbs	658	658	658
Coarse Aggregate, lbs	803 (15 ft^3 @ 53.5 pcf)	885 (15 ft^3 @ 59 pcf)	788 (15 ft^3 @ 53 pcf)
Fine Aggregate, lbs	1091 (16 ft^3 @ 68.2 pcf)	514 (8.5 ft^3 @ 67.5 pcf)	None
Colorado River Sand, lbs	None	733 (8.5 ft^3 @ 86.2 pcf)	1458 (18 ft^3 @ 81 pcf)
Water (theoretical),* lbs	250	250	250
Air Entraining Agent** (Airsene), oz	2.5	2.5	2.5
Unit Weight, pcf	112	115	118

*Water added to produce 6 in. slump.

**Air content about 6 percent for all mixes.

(d) Other Variables--Lightweight Concrete Series. Seven tests were conducted using 90° standard hooks conforming to ACI 318-71 [4] specifications, and one test was conducted with a 180° hook. All specimens had a 2-7/8 in. concrete cover over the anchored bars (Type 1 confinement in Ref. 1). One specimen was cast with #3 ties through the joint at 5 in. c.c. in addition to the standard 2-7/8 in. concrete cover over the anchored bars (Type 3 confinement), and the remainder had no ties through the joint. Previous tests concluded that the effect of column axial load on hooked bar strength was negligible for cases where the tail extension of the hook was oriented in the direction of the axial load. One specimen of this series was loaded with an axial load which produced an average compressive stress of about 3000 psi (H). All other specimens (including the lead embedment series) were subjected to axial stress of about 800 psi (L).

2.1.3 Specimen Instrumentation. Comparison between specimens was made using curves of stress versus slip of the anchored bars relative to the concrete. To measure slip, the procedure developed by Minor and Jirsa [3] was used.

At the point where slip was to be measured, a 0.059 in. diameter piano wire was attached to the bar by making a short 90° bend at the end of the wire and inserting it into a hole of equal diameter drilled in the bar. Figure 2.2 shows the five slip measurement points along the length of the anchored bars: point 1H at the front face of the specimen (called "lead" slip); point 2H at the point of horizontal tangency of the bent portion of the hook; points 3H and 3V at the point of vertical tangency; and 4V at the end of the tail of the hook. The slip wires were long enough to reach through the form at the back face of the specimen. The wires were oriented in the direction displacement was to be measured at the points of connection to the anchored bars.

After a slip wire was attached to the bar, a plastic tube was placed over the entire length of the wire to prevent bond. A small amount of rubber sealer was placed at the connection between the wire

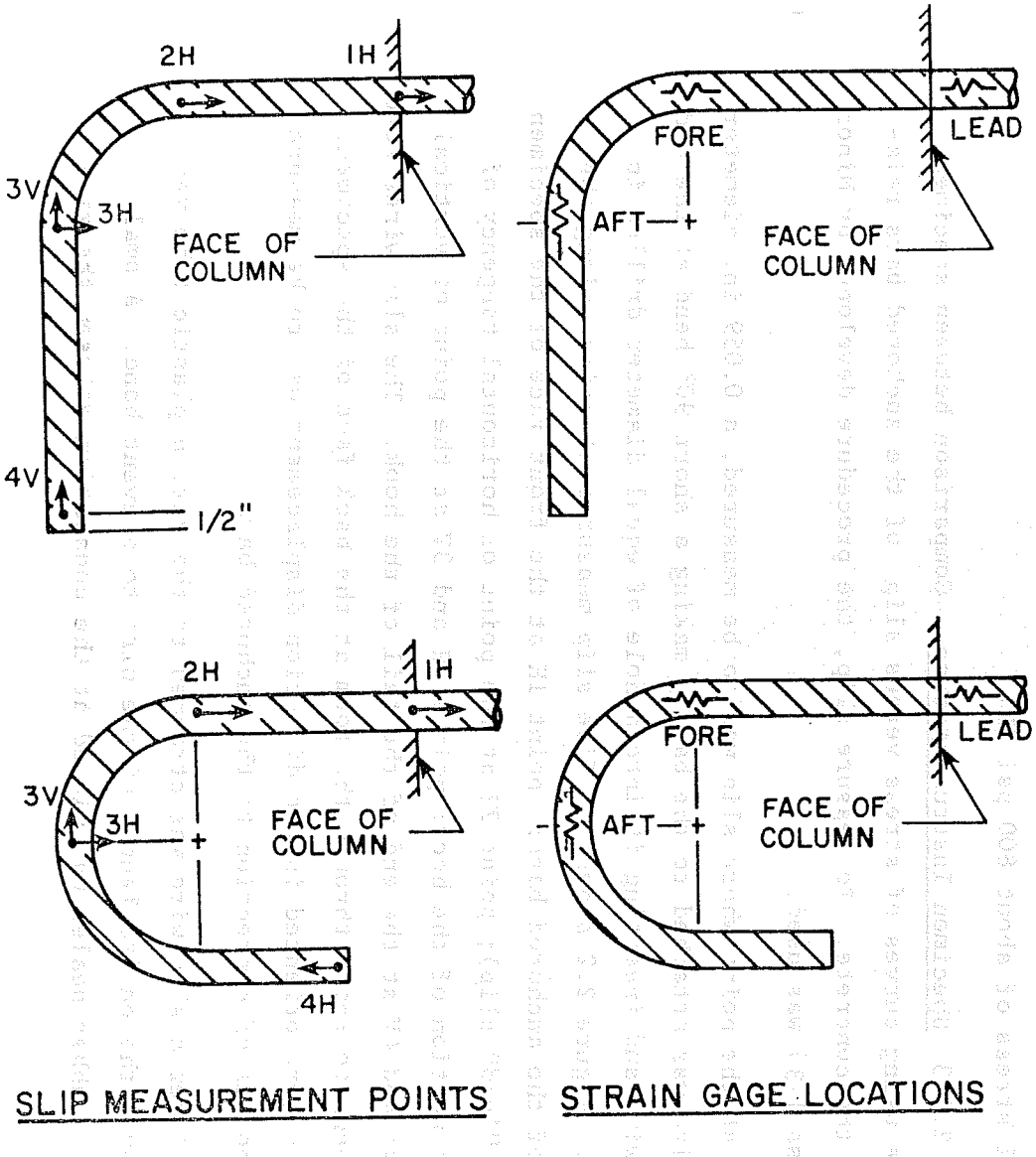

Fig. 2.2 Instrumentation

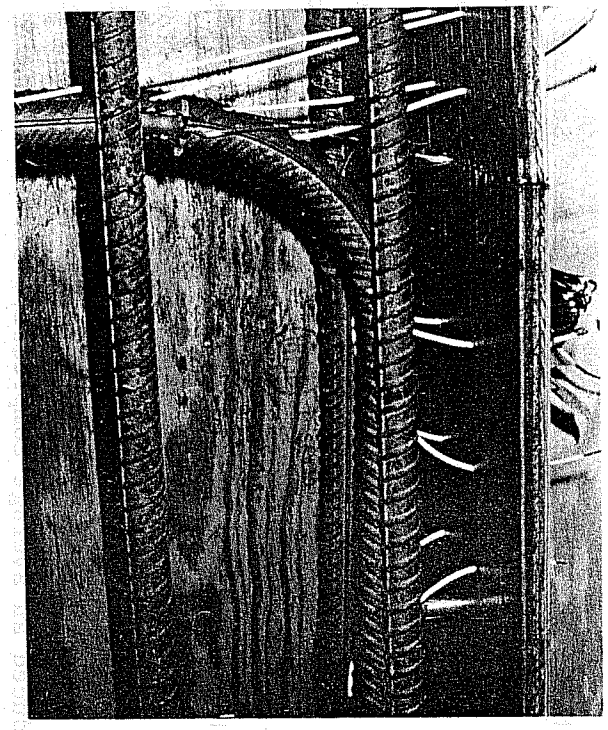

Fig. 2.3 Slip wires attached to bars

and the anchored bar to seal the tube and to allow movement of the wire in the direction it was expected to travel. It was extremely important to use this sealer to prevent interlock between the protruding wire and the concrete. The loss of bond between the anchored bar and the concrete at the point of attachment of the slip wires was considered negligible. Figure 2.3 shows the wires and tubing in place on a specimen in the form prior to casting.

To reduce the wobble of the slip wire in the tube, the wire was placed in tension using a spring between the concrete surface and a small brass plug fastened to the wire with a set-screw. This spring put a tensile load of approximately 3 to 4 lb on the wire. A linear displacement potentiometer was used to measure movement of the wire and was attached to the back face of the column using a metal frame constructed from electrical conduit pipe. This frame was clamped to two threaded rods screwed into inserts placed in the specimen at the time of casting. The potentiometers were read by using a digital voltmeter. Results of the hooked bar anchorage study indicated that the back face was uncracked until failure was imminent, and provided a good reference plane for slip measurement.

To determine the stresses in the anchored reinforcing bars, three strain gages were mounted on each bar. Figure 2.2 shows the location of these gages. One gage was located outside the front face of the specimen and monitored "lead" bar stress. A second gage was mounted at the point of horizontal tangency (fore) of the bent portion of the hook, and the third gage was located at the point of vertical tangency (aft). The application of strain gages provided a means of estimating the stress transferred from the bars to the concrete along various portions of the bars. Bond reduction was negligible in the region of the gages where an area of approximately 1/2 in. by 1-1/2 in. was waterproofed.

2.1.4 Fabrication of Specimens. Instrumentation of the anchored bars was completed before placing them into the form. The bars were prepared by (1) cutting the bars to proper length, (2) drilling holes

for slip wires, (3) preparing the bars for strain gages, (4) mounting and waterproofing strain gages, and (5) mounting and sealing slip wires.

Plywood forms were constructed to allow casting specimens in a vertical position. Two specimens were prepared and cast at one time.

2.2 Loading System

The forces applied to the test specimens are shown in Fig. 2.1. The loading of the specimens was intended to approximate the forces on the joint in a typical frame. The loading frame was constructed to apply axial load on the column, and tensile and compressive beam forces on the joint. The frame is shown in Fig. 2.4.

2.2.1 Axial Loading. To load the column, four 100-ton centerhole hydraulic rams were placed above the top axial loading head. Alloy steel rods, 2 in. in diameter, were passed through the rams, the top loading head, along the sides of the specimen, and through the bottom platform. Two of the four rods were instrumented with strain gages and served as load cells to monitor axial load. Hydraulic oil pressure was also monitored. The top and bottom loading heads were fabricated using a series of channels to provide a rigid loading surface and to distribute the load uniformly over the column section. In addition, a quick setting plaster was used between the specimen and loading surfaces to ensure uniform load distribution.

2.2.2 Anchorage Loading. The anchored beam reinforcing bars protruded from the specimen about 6 ft. to allow for installation of equipment to provide a tensile loading to the bars.

A vertical reaction beam composed of two 18 in. deep steel channels was erected about 20 in. from the front of the specimen, as shown in Fig. 2.4. This beam was mounted on an axle at the base of the loading frame. The anchored beam reinforcing bars passed between the two channels. Two 60-ton centerhole rams were placed over the bars to apply tensile load. A 5-in. Cadweld sleeve was attached to each bar immediately beyond the loading rams (see Fig. 2.4). The sleeves provided convenient loading collars

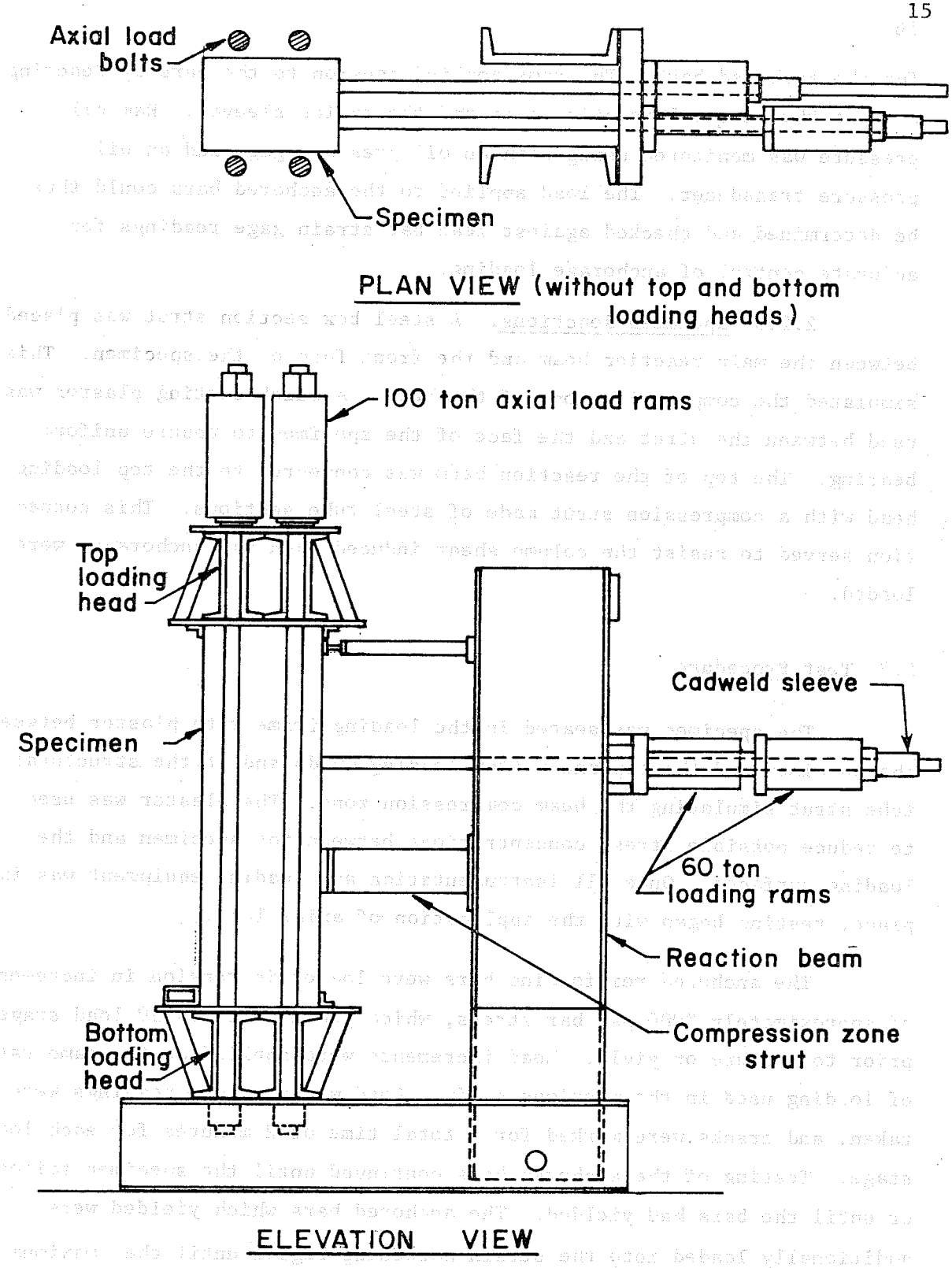

Fig. 2.4 The loading frame

for the anchored bars. The rams applied tension to the bars by reacting against the vertical reaction beam and the splice sleeves. Ram oil pressure was monitored using both an oil pressure gage and an oil pressure transducer. The load applied to the anchored bars could thus be determined and checked against lead bar strain gage readings for accurate control of anchorage loading.

2.2.3 Specimen Reactions. A steel box section strut was placed between the main reaction beam and the front face of the specimen. This simulated the compression zone of the beam. A quick setting plaster was used between the strut and the face of the specimen to ensure uniform bearing. The top of the reaction beam was connected to the top loading head with a compression strut made of steel tube sections. This connection served to resist the column shear induced when the anchorages were loaded.

2.3 Test Procedure

The specimen was seated in the loading frame with plaster between the specimen and the top and bottom loading heads and at the structural tube strut simulating the beam compression zone. The plaster was used to reduce possible stress concentrations between the specimen and the loading surfaces. Once all instrumentation and loading equipment was in place, testing began with the application of axial load.

The anchored reinforcing bars were loaded in tension in increments of approximately 2000 psi bar stress, which provided 20 to 30 load stages prior to failure or yield. Load increments were applied at the same rate of loading used in the previous study. Load was applied, readings were taken, and cracks were marked for a total time of 2 minutes for each load stage. Testing of the anchored bars continued until the specimen failed or until the bars had yielded. The anchored bars which yielded were additionally loaded into the strain-hardening region until the maximum stroke, about 3 in., of the hydraulic ram was reached.

3. TEST RESULTS

3.1 Introduction

The slip and strain measurements at the points shown in Fig. 2.2 are plotted against measured lead bar stress, the stress at the face of the column measured from hydraulic pressure to the rams loading the bars. Figure 3.1 shows a plot of lead bar stress versus slip, and Fig. 3.2 shows measured stress from strain measurements plotted against lead bar stress. These figures are plotted from data measured for Specimen 11-18 and are typical of the trends observed for all specimens tested in this program. Measured data for all tests are presented in Refs. 6 and 7.

3.2 Lead Embedment Series

Lead stress-lead slip (at point 1H) curves are shown in Fig. 3.3 for #9 bars and in Fig. 3.4 for #11 bars. For each curve, average values for the two bars of a specimen are plotted. In addition to the curves for this series of tests, curves are plotted in Fig. 3.4 for two additional specimens from data extracted from a previous study on hooked bar anchorage by Jirsa and Marques [1]. In addition to the observations noted in this present study, findings from the previous study will also be included and used later in this presentation to develop design recommendations.

As can be seen in Fig. 3.3, Specimens 9-15 and 9-21 each failed at a strength less than that of specimens with smaller lead embedment length. These specimens had concrete strengths of 3800 psi and 3600 psi, less than the 4500 psi specified. Figure 3.3 also shows a large increase in lead slip with a small increase of stress. It was observed that at equal levels of lead bar stress the stress measured at the points of tangency of the hooks are nearly equal to each other and also to the measured lead bar stress. These observations tend to indicate that no

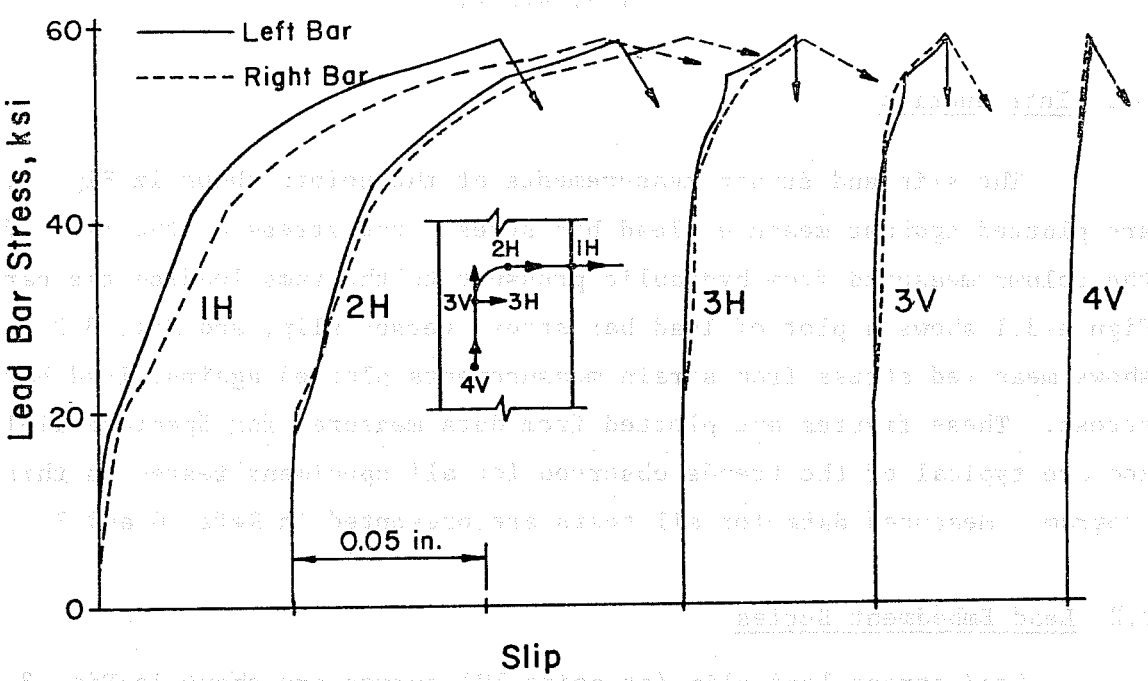

Fig. 3.1 Measured stress-slip relationships, Specimen 11-18.

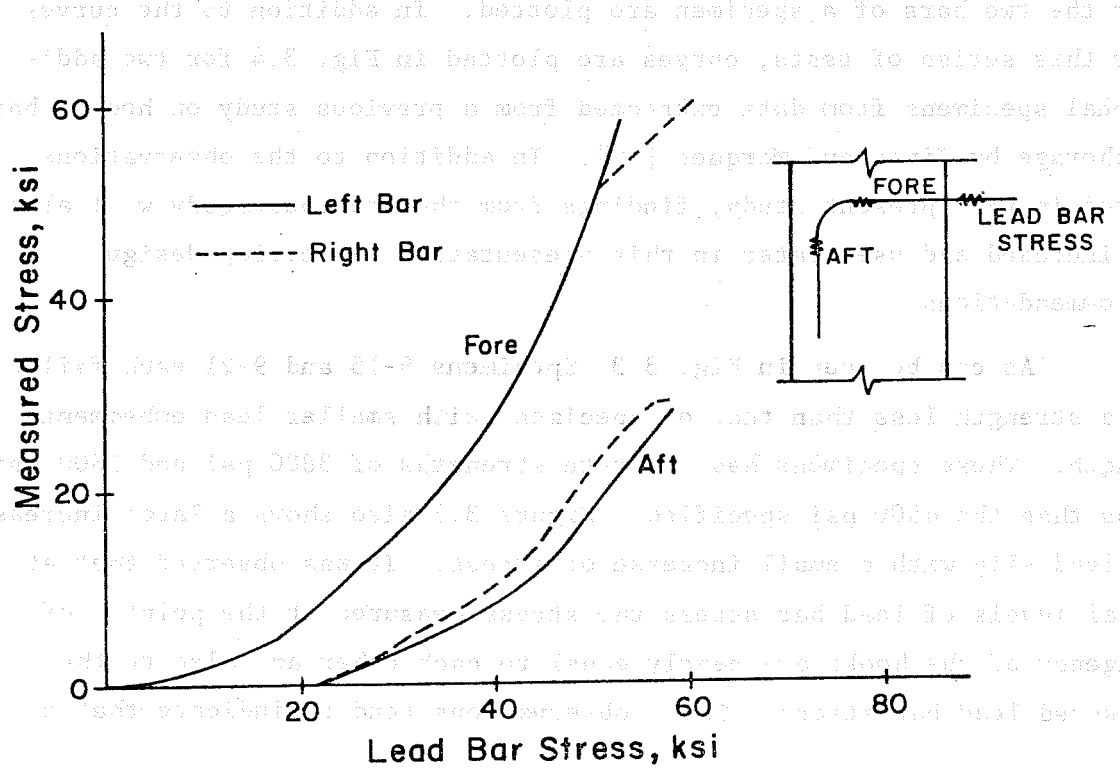

Fig. 3.2 Measured stresses--Specimen 11-18

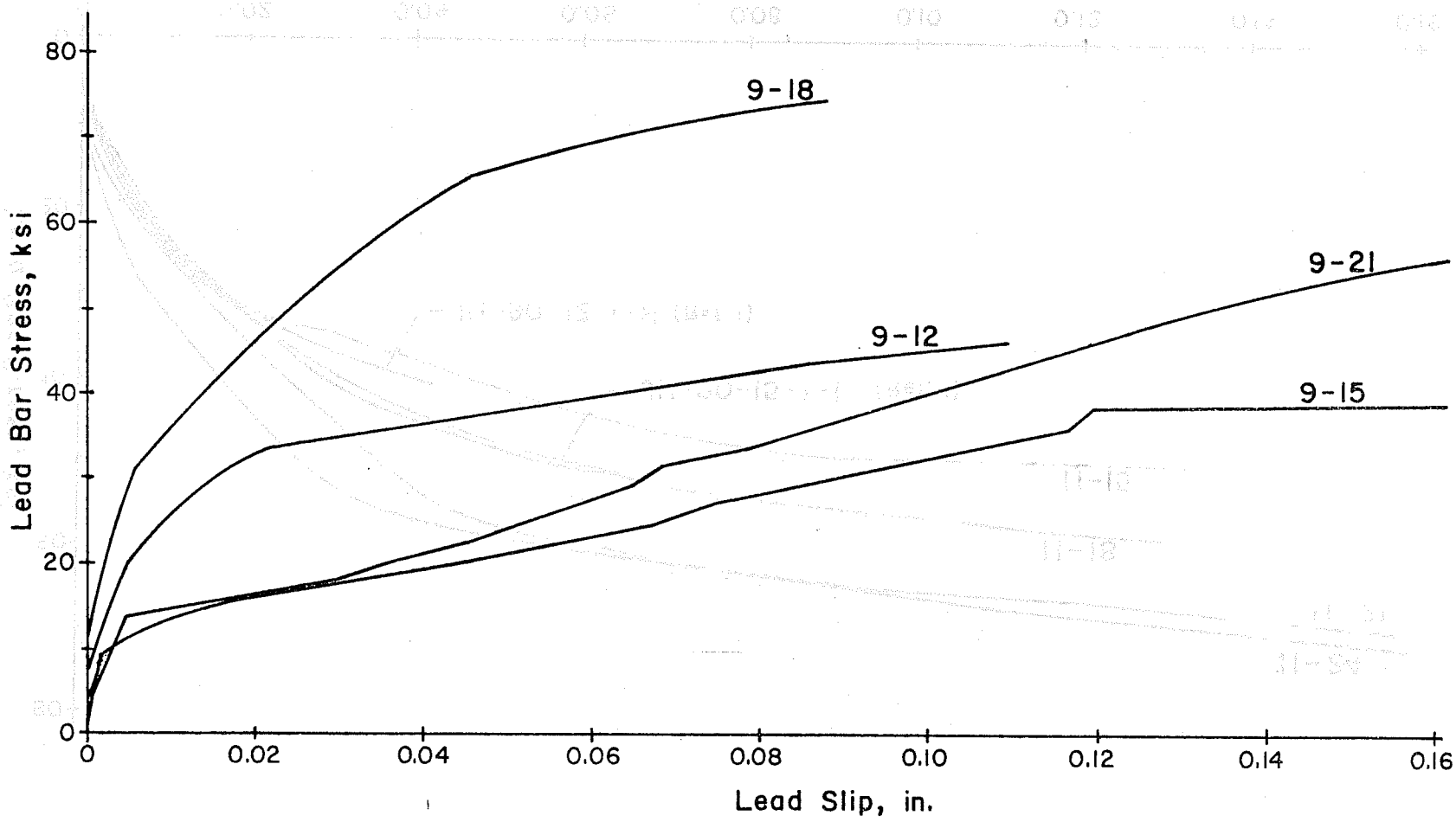

Fig. 3.3 Influence of lead embedment on slip for #9 bars

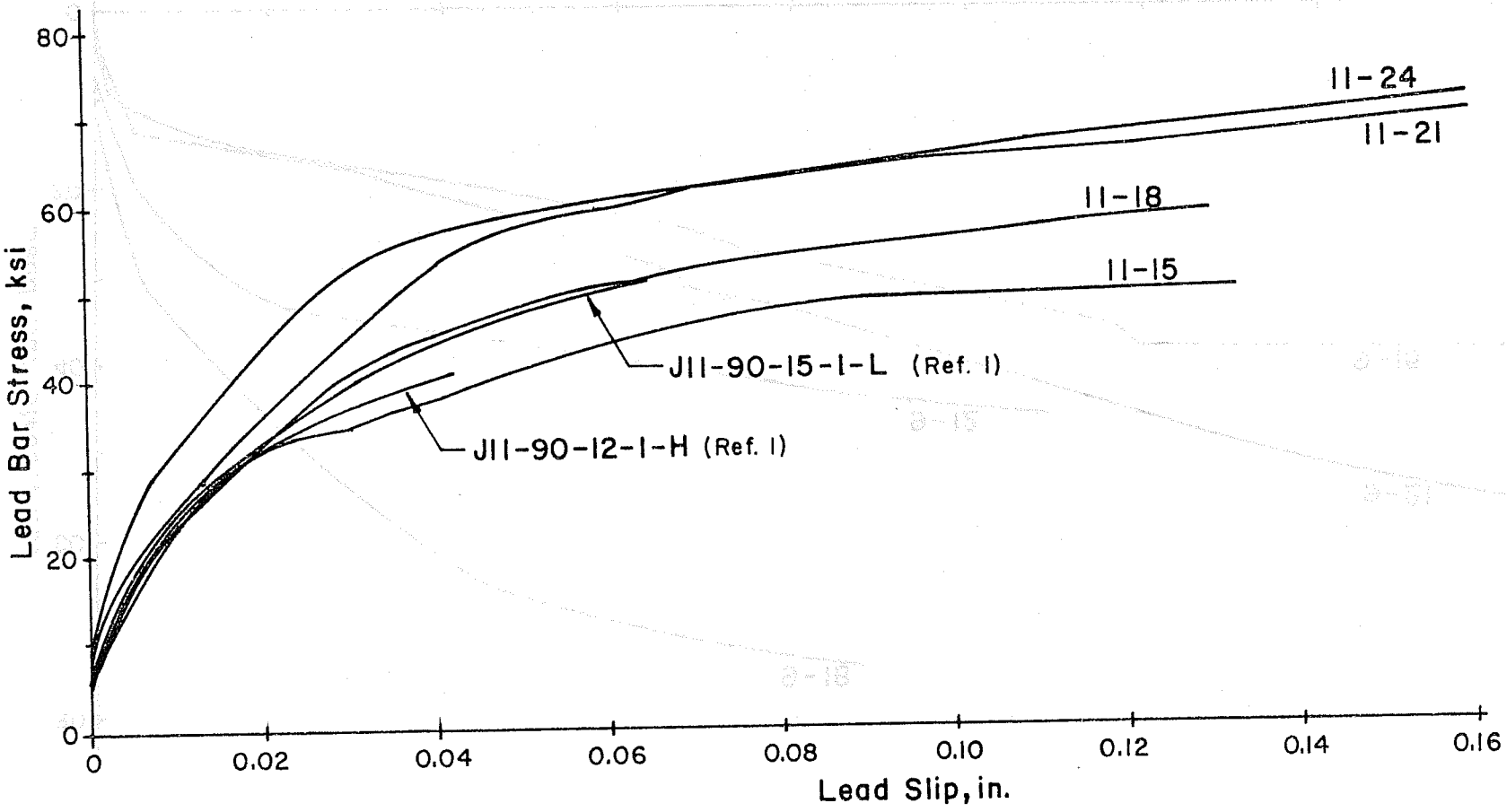

Fig. 3.4 Influence of lead embedment on slip for #11 bars

stress was being transferred along the straight bar embedment to the concrete. After failure, the side cover was removed and yellowish-brown powder was observed beneath the anchored bars. Very little of the aggregate was broken, indicating it had not bonded well with the cement paste. The lack of bonding and residue beneath the bars was attributed to poorly washed aggregages used in the concrete. Although the two specimens cannot be compared directly with other specimens, they can be compared with each other.

The following general trends were observed in the test results:

(1) Most of the slip occurs along the straight lead embedment and the curved portion of the hooked bar. Very little slip was measured on the tail extensions of the hooks. In each case, the lead slip (point 1H) is the largest. If the straight lead embedment were not sufficient to develop yielding of the anchored bars, the slip at point 2H was nearly as large as the lead slip. The slip at points 3H and 3V was very small in all cases, and no significant slip was measured at point 4V until failure was imminent.

(2) The initial stiffness (stress divided by slip, up to levels of about 30 ksi lead stress) decreased as the bar size was increased. There was a slight but not very significant increase in initial stiffness as the lead embedment length was increased.

(3) At stress levels above 30 ksi, the stiffness was significantly less than the initial stiffness, and the effect of the increased length in straight lead embedment became apparent. For #11 bars at a given value of slip, the increase in strength was about 10 ksi for each 3 in. increase in embedment length until the yield stress of the bar was reached.

(4) The stress transferred from the anchored bar to the concrete along the straight lead embedment (the difference between the lead bar stress and the stress at the start of the hook) was significant at lead bar stresses less than 30 ksi, but decreased rapidly as the specimens neared failure.

(5) In nearly all the tests the stress in the tail extension was generally small, less than 20 ksi until failure was imminent. Near failure stresses on the tail increased rapidly, but this increase may represent some effects of flexure due to the bar slipping as the concrete splits.

3.2.1 Influence of Lead Embedment Length on Slip. It is apparent that the strength and stiffness of the hooked anchorages are significantly affected by the lead embedment or by the thickness of the column. The #11 bars embedded in 12 X 21 in. and 12 X 24 in. columns reached stresses well over the yield stress of the steel before the tests were terminated. The bars in a 12 X 18 in. column reached a stress near yield before failure of the concrete, and those in a 12 X 15 in. column reached 50 ksi.

In general, the longer lead embedment lengths result in higher stresses at failure, and the slip is greater at all stress levels with shorter lead embedment. A summary of measured slip behavior is listed in Table 3.1. Lead stresses at lead slips of 0.005, 0.016, and 0.05 in. are listed. In addition, slip at point 1H under applied bar stresses of 0.6 of the computed anchorage strength using the provisions of ACI 318-71 [4] is given. Slip and stress at failure are also tabulated. Stress at a slip of 0.016 in. was selected because it is in the range suggested as a permissible crack width in beams in the ACI 318-71 Commentary [5]. If it is assumed that the crack width at the beam-column joint is about equal to the slip of the anchored bar, the observed stress at 0.016 in. slip provides a measure of the serviceability of the hooked bar. In a similar manner, slip values at a level of 0.6 of yield correspond to the provisions in Sec. 10.6.3 of ACI 318-71 [4] for computing crack width at service loads. In general, stresses at 0.005 in. slip were about 20 ksi, at 0.016 in. slip about 30 ksi, and at 0.05 in. slip, between 40 and 50 ksi. Only in specimens which fail at stresses higher than yield

TABLE 3.1 SUMMARY OF MEASURED SLIP BEHAVIOR--LEAD EMBEDMENT SERIES

Specimen	Stress at Lead Slip of			Lead slip at $0.6(f_h + f_\ell)$ Lead Stress in.	Approx. Slip at Failure in.	Stress at Failure in.
	0.005 in. ksi	0.016 in. ksi	0.05 in. ksi			
9-12	20	31	38	0.010	0.12	47
9-15	12	15	21	0.072	0.21	43
9-18	28	41	67	0.008	0.09	74
9-21	14	16	24	0.068	0.20	59
11-15	19	30	41	0.009	0.13	50
11-18	18	29	48	0.011	0.13	58
11-21	17	33	58	0.012	0.24	73
11-24	25	39	59	0.005	0.25	77

stresses of the anchored bars do the stresses at the specified slip levels begin to increase.

3.2.2 Influence of Lead Embedment Length on Stress Characteristics. The stress measured at the start of the hook is plotted against the measured lead bar stress in Figs. 3.5 and 3.6. Figure 3.5 shows curves for #9 bars, and Fig. 3.6 shows #11 bars. Curves are plotted in Fig. 3.6 for two additional specimens from Ref. 1. It must be kept in mind that as the bars pulled out, bending stresses were induced on the bars near the bend, and at large slips the stresses measured at the start of the hook can only be considered approximate. Stresses greater than lead bar stresses, shown as dashed lines in Figs. 3.5 and 3.6, are attributed to bending stresses in the bars.

At a given level of stress, the difference between the lead bar stress and the stress at the start of the hook may be considered as the amount of stress that is transferred to the concrete by the straight lead embedment. As can be seen in Figs. 3.5 and 3.6, in the specimens with short lead embedment much less stress was transferred along the straight bar portion than in specimens with longer lead embedment. For the specimens which exceeded the yield stress of the anchored bars, the stress transferred was large up to stresses of about 30 ksi and began to decrease somewhat as additional load was applied to the bars. For the specimens which failed before reaching yield stress of the bars, the stress transfer increased only up to lead bar stresses of 10 to 20 ksi and then decreased rapidly as the specimens neared failure. At failure, the stress at the start of the hook in many of the specimens was nearly equal to the lead bar stress, indicating that no stress was being transferred along the entire lead embedment length.

3.2.3 Mode of Failure. In early all the tests the general performance and crack formation followed a similar pattern. As tensile load was applied to the anchored bars, the first cracking was located in the front face of the specimen radiating out from the anchored bars. The vertical cracks developed most rapidly and eventually terminated in the

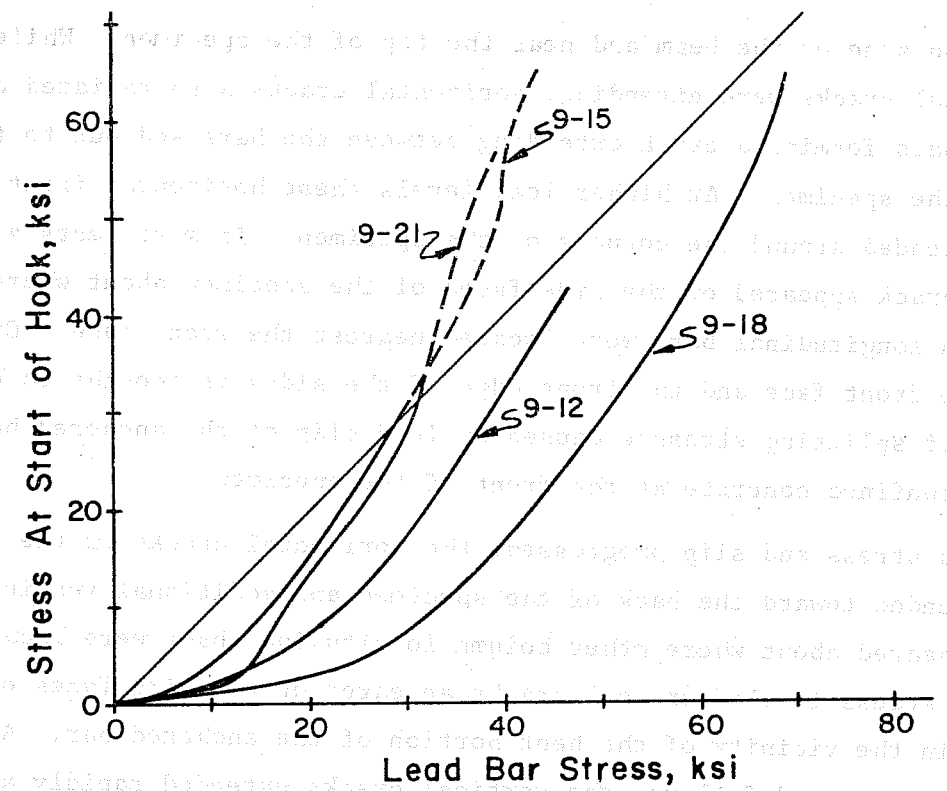

Fig. 3.5 Influence of lead embedment on stresses for #9 bars

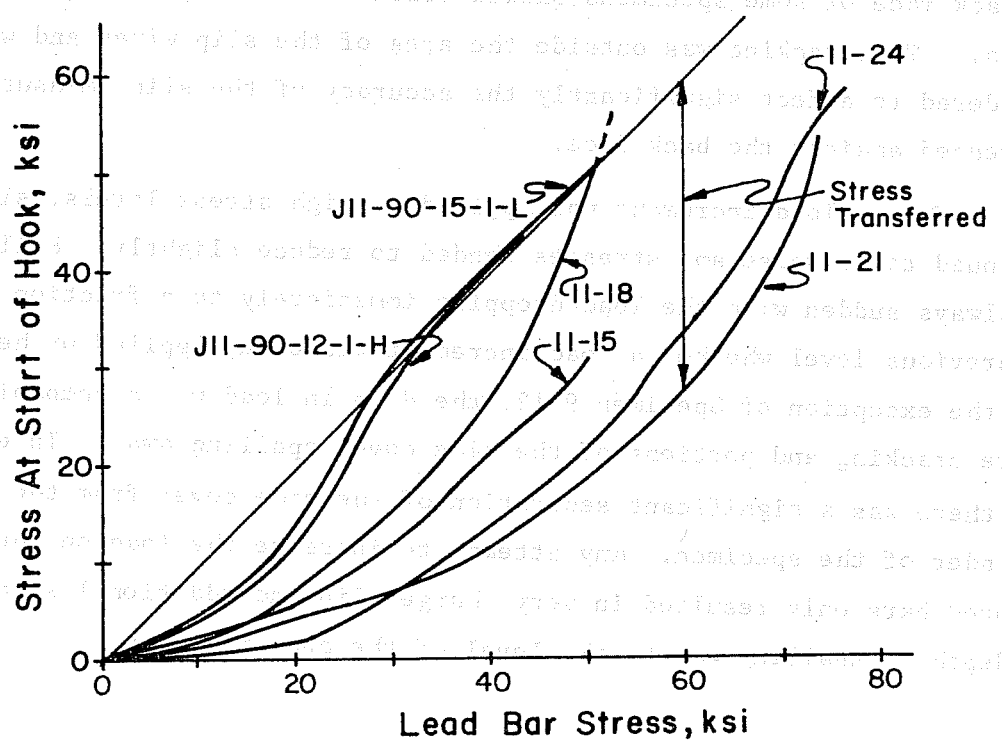

Fig. 3.6 Influence of lead embedment on stresses for #11 bars

compression zone of the beam and near the top of the specimen. While the vertical cracks were extending, horizontal cracks also radiated out from the bars forming a crack extending between the bars and out to the edges of the specimen. At higher load levels these horizontal front face cracks extended around the corners of the specimen. In most tests a vertical crack appeared on the side faces of the specimen about where the column longitudinal bars were located nearest the front face. Cracking of the front face and the front edge of the sides is thought to be a result of splitting stresses caused by lead slip of the anchored bars in the unconfined concrete at the front of the specimen.

As stress and slip progressed, the horizontal cracks on the side faces extended toward the back of the specimen and additional vertical cracks appeared about where other column longitudinal bars were located. At higher stress levels vertical cracks appeared on the side faces of the specimen in the vicinity of the bent portion of the anchored bar. As the specimens neared failure, the vertical cracks extended rapidly above and below the level of the anchored bar in a slightly inclined direction. The back face of some specimens showed vertical cracking at high load levels. The cracking was outside the area of the slip wires and was not considered to affect significantly the accuracy of the slip measurements referenced against the back face.

When a load increment was applied at high stress levels, slip continued to increase and stresses tended to reduce slightly. Failure was always sudden with the load dropping immediately to a fraction of its previous level whether a load increment was being applied or held. With the exception of Specimen 9-12, the drop in load was accompanied by severe cracking and portions of the side cover spalling away. In each case there was a significant separation of the side cover from the remainder of the specimen. Any attempt to increase the load on the anchored bars only resulted in very large slip and additional separation. The depth of spalling was to the level of the anchored bars.

Specimen 9-12, which had the shortest straight lead embedment length, developed a severe diagonal crack extending up from the hooked portion of the anchored bar to the top front face of the specimen and also down to the compression zone of the beam. At failure the crack opened toward the front of the specimen. No spalling or separation of the sides could be observed. Specimen 9-12 is the only test in this series or those of Ref. 1 in which shear could be considered a contributing factor in producing failure.

3.3 Lightweight Concrete Series

From the data for the lightweight concrete tests, the following trends were observed. These trends are similar to those noted in the lead embedment series using normal weight concrete.

(1) Most of the slip occurs over the lead embedment and the curved portion of the hooked bar. Very little slip was measured on the tail extensions of the hooks. In all cases the lead slip (location 1H) is the greatest. The bars that did not yield exhibited slip at the start of the bend (location 2H) of approximately the same magnitude as the lead slip near failure. Slip at the end of the bend (locations 3H and 3V) was significantly smaller and in most specimens slip at the end of the tail extension (locations 4H or 4V) was negligible until high levels of stress were attained and failure was imminent.

(2) The initial stiffness defined as stress divided by slip for the initial portion of the curves decreased as bar size increased.

(3) The measured slip at location 4H on the specimen with the 180° hook indicated that the entire hook was being pulled towards the front of the specimen rather than around the bend.

(4) Stress transfer along the straight lead embedment (the difference between the lead bar stress and the stress at the start of the curved portion of the hook) was negligible as the specimen reached failure for #11 bars. For #7 bars at lead bar stresses of 40 to 50 ksi,

the stress transferred varied from 20 to 40 ksi, but decreased rapidly as the specimen approached failure.

(5) Stresses measured at the tail extension were generally small. Near failure, stresses on the tail extension increased very rapidly while the magnitude of the slip at this location remained very small.

A summary of measured slip behavior is presented in Table 3.2. Values of slip and stress at the same reference points used in Table 3.1 are included here.

To evaluate the influence of the individual parameters considered in the lightweight concrete series the stress and slip data for comparable tests will be discussed in detail. Slip data presented are for the lead slip only.

3.3.1 Influence of Hook Geometry. Figure 3.7 presents lead bar stress versus lead bar slip curves for four specimens, two of 50 percent replacement lightweight concrete and two of normal weight concrete. These curves represent specimens in which lateral confinement remains constant but bend geometry varies. As reported in Ref. 1, there is little significant difference in the strength of 90° and 180° hooks. However, slip for the lightweight specimens is significantly greater.

3.3.2 Influence of Confinement. The effect of #3 closed ties through the joint at 5 in. c.c., referred to as Type 3 confinement, versus no ties through the joint, referred to as Type 1 confinement, can be seen in Fig. 3.8. The two lower curves represent specimens from this test program (FR--50 percent fines replaced), and the two upper curves are companion normal weight specimens from Ref. 1. The inclusion of ties through the joint on the two normal weight concrete specimens shows an increase of about 19 percent in the ultimate stress. It can also be seen that to obtain this increase in strength approximately 50 percent increase in slip was required. The two 50 percent replacement lightweight concretes behaved similarly; strength was increased by

TABLE 3.2 SUMMARY OF MEASURED SLIP BEHAVIOR--LIGHTWEIGHT CONCRETE SERIES

Specimen	Stress at Lead Slip of			Lead Slip at (0.6) Anchorage Strength Computed Using ACI		Lead Slip at (0.6) Anchorage Strength Measured in.	Approx. Slip at Failure in.	Lead Stress at Failure in.
	0.005 in. ksi	0.016 in. ksi	0.050 in. ksi	with C Factor	w/o C Factor			
11-90-1-L-AL	18	29	38	0.006	0.006	0.012	0.10	44
11-90-1-H-AL	15	29	40	0.008	0.009	0.014	0.09	46
11-90-1-L-AS	25	33	44	0.003	0.004	0.012	0.10	52
11-90-1-L-FR	13	21	31	0.015	0.016	0.019	0.11	38
11-180-1-L-FR	16	24	34	0.010	0.011	0.015	0.11	38
11-90-3-L-FR	12	21	35	0.016	0.018	0.030	0.16	47
7-90-1-L-AS	34	60	73	0.006	0.007	0.011	0.12	82
7-90-1-L-FR	37	45	66	0.004	0.005	0.021	0.16	80

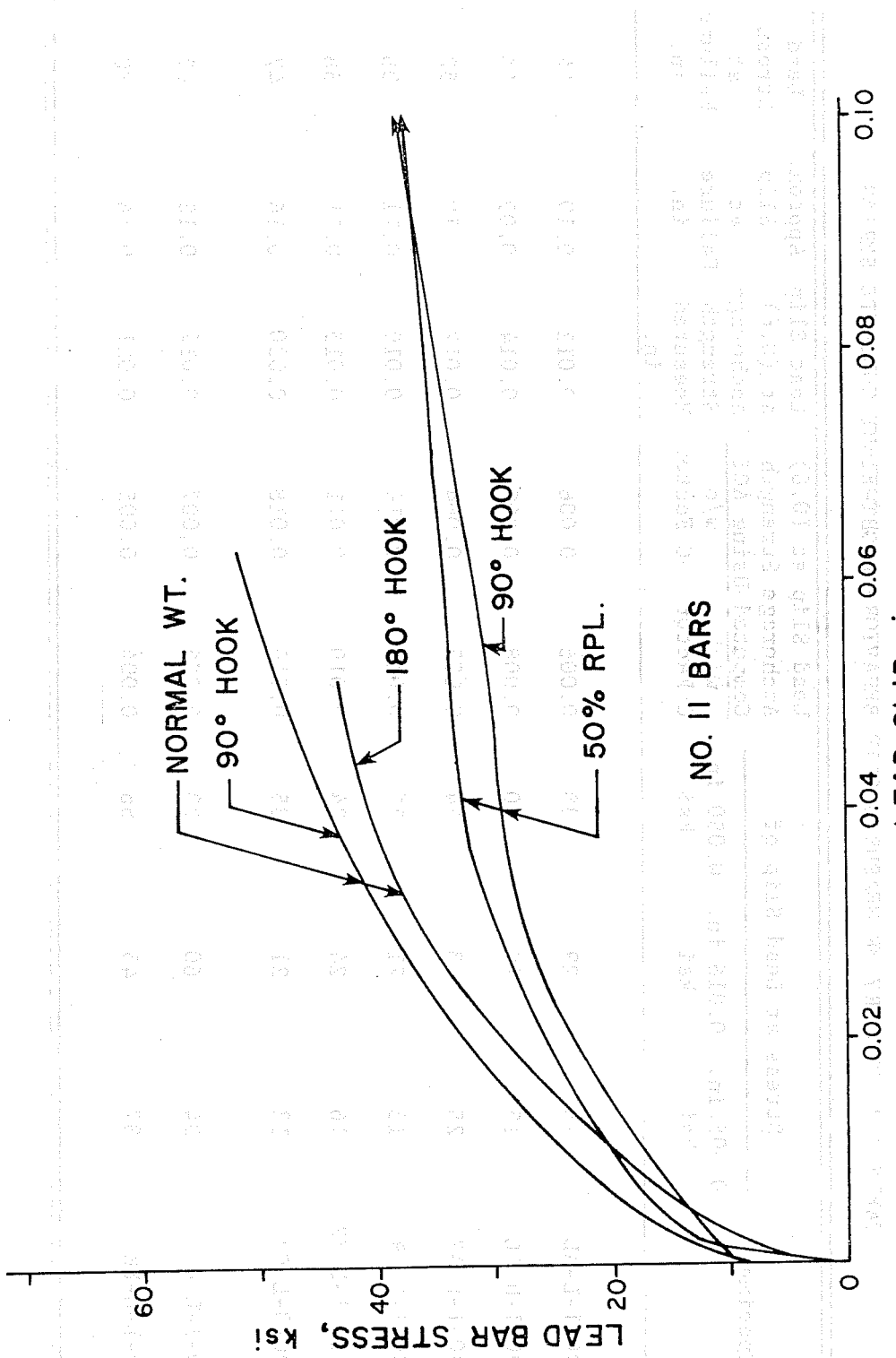

Fig. 3.7 Influence of hook geometry on slip

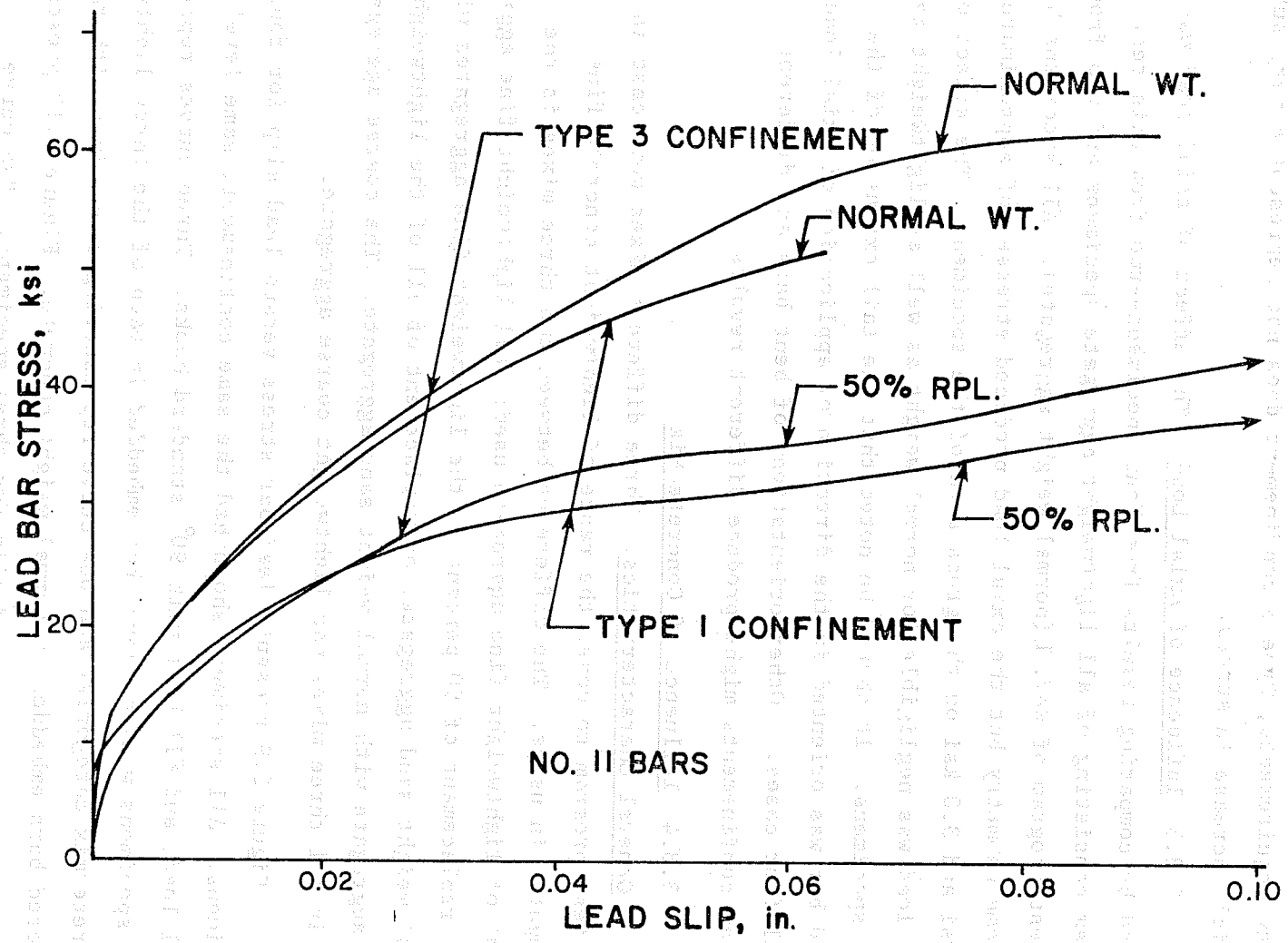

Fig. 3.8 Influence of confinement on slip

approximately 23 percent and it required about a 40 percent increase in slip to attain the higher strength. At this point it should be noted that in a range of slip that is more reasonable with respect to serviceability requirements, Type 3 confinement does not represent a very substantial increase in stress.

3.3.3 Influence of Axial Load. The effect of axial load was studied by comparing results from four specimens--two from this test program consisting of all lightweight aggregate specimens and two from the test program of Ref. 1 (normal weight aggregate). All specimens had the same geometry but the axial load produced stresses of approximately 0.8 ksi and 3.0 ksi on the gross area of the specimens. The effect of axial load was negligible for normal weight as well as lightweight concrete specimens. It should be noted that the tail extension of the hooked bar was oriented in the direction of application of axial load in all four cases. Other orientations of bent bars and different lateral confinements might produce different results.

3.3.4 Influence of Concrete Mix

General Characteristics. Three different mixes were cast in this test program to cover the range of lightweight concrete fine aggregates in usage. The difference between the three mixes is the amount of lightweight fine aggregate used: all lightweight fine aggregate, replacement of 50 percent of the lightweight fine aggregates with normal weight sand aggregate, or replacement of all of the lightweight fine aggregate with normal weight sand aggregate. The coarse aggregate used in all three mixes was lightweight coarse aggregate.

Figure 3.9 presents lead bar stress versus lead slip for four specimens. All specimens shown had the same confinement, same level of axial load, and #11 bars with 90° standard hooks. Three curves represent specimens with anchored bar embedded in each of the three lightweight concrete mix categories and one curve representing a specimen with the anchored bars embedded in normal weight concrete. Figure 3.10 presents lead bar stress versus lead slip for three specimens. Two curves

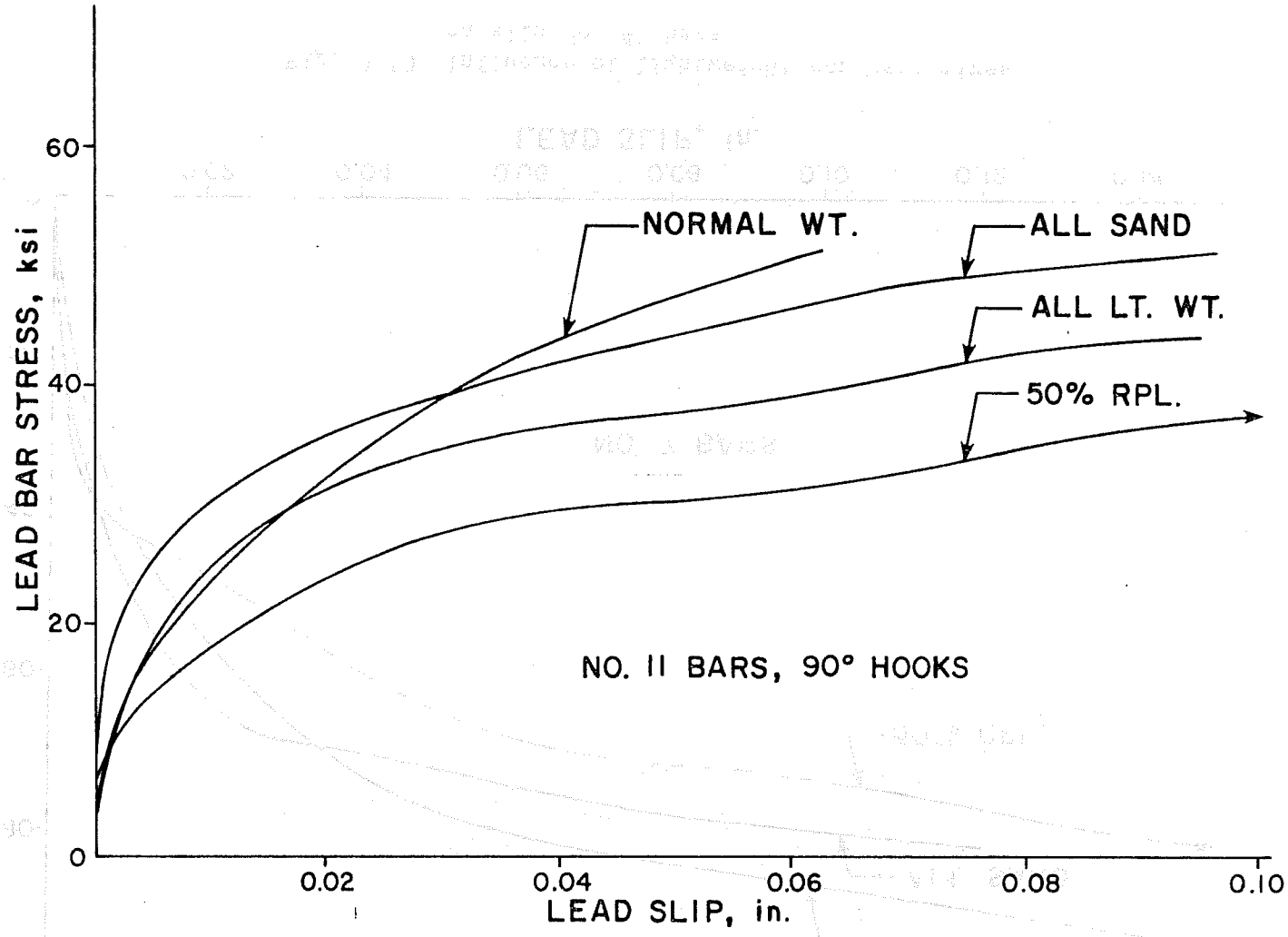

Fig. 3.9 Influence of lightweight concrete mixes on slip for #11 bars

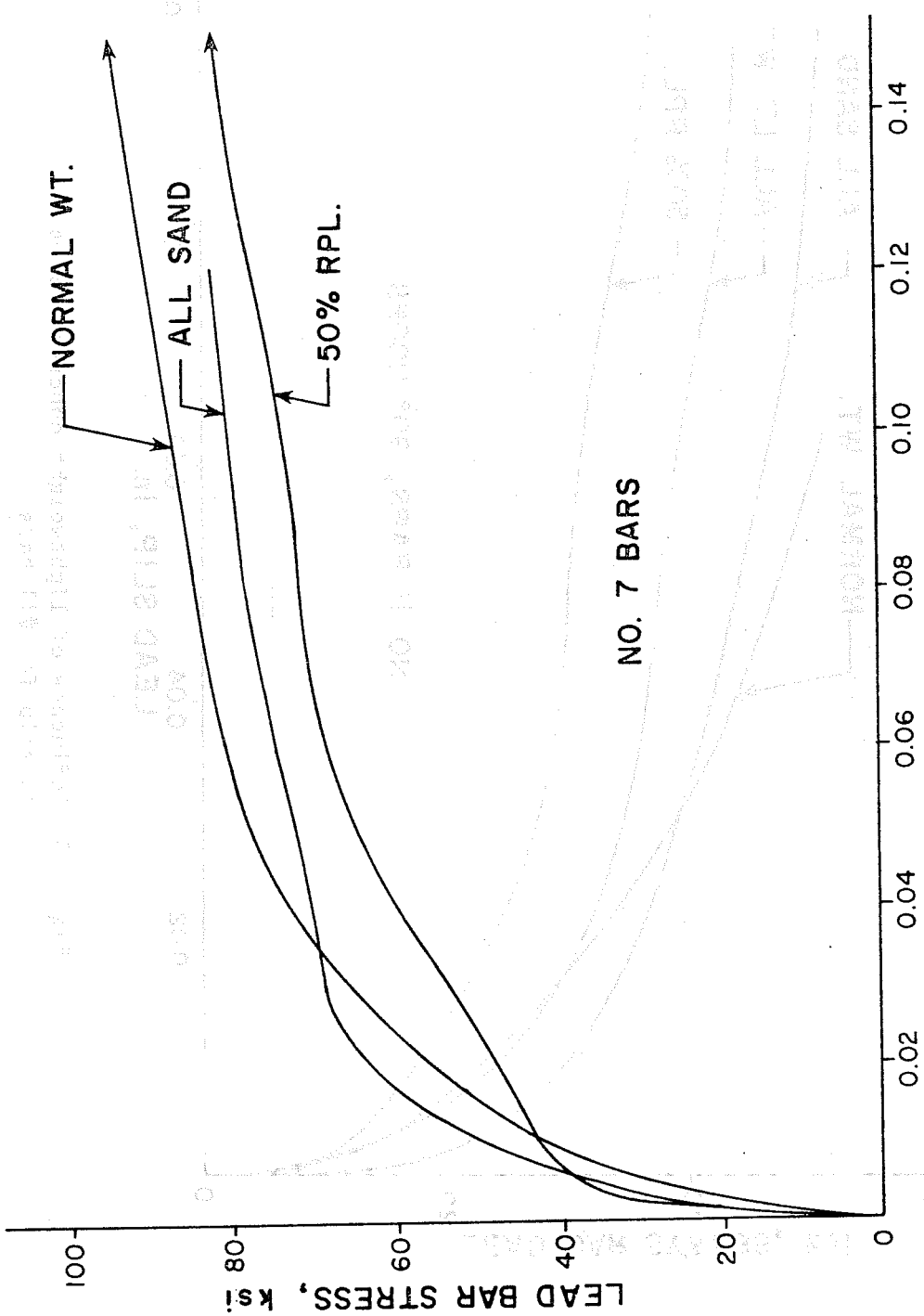

Fig. 3.10 Influence of lightweight concrete mixes on slip for #7 bars

represent specimens with #7 bars in two of the lightweight concrete mix categories from this test program, and one specimen with #7 bars anchored in normal weight concrete.

All-Lightweight Concrete. Referring to Fig. 3.9, it can be seen that the all-lightweight concrete specimen reached approximately 85 percent of the ultimate stress attained by the normal weight concrete specimen. It also can be seen that at failure the all-lightweight concrete specimen exhibited approximately 50 percent more slip than the normal weight specimen.

Fifty Percent Replacement. Figure 3.9 shows that the 50 percent replacement concrete specimen reached approximately 75 percent of the ultimate stress attained by the normal weight concrete specimen. Also, it can be seen that the 50 percent replacement concrete specimen showed approximately 80 percent more slip at failure than the normal weight specimen. Figure 3.10 shows that the 50 percent replacement concrete specimen reached approximately 82 percent of the ultimate stress attained by the normal weight concrete specimen. However, it should be noted that the shape of the curve is dictated mainly by yielding and strain hardening of the anchored bar rather than crushing of the concrete. The slip at failure of the 50 percent replacement concrete specimen is roughly equivalent to the slip of the normal weight specimen at failure.

All-Sand Lightweight Concrete. Figure 3.9 shows that the all-sand lightweight concrete specimen reached roughly the same ultimate stress attained by the normal weight concrete specimen. It also shows that at failure the all-sand lightweight concrete specimen exhibited approximately 50 percent more slip than the normal weight concrete specimen. Figure 3.10 shows that the behavior of the all-sand lightweight concrete specimen was very similar to the normal weight concrete specimen throughout the range of loading. It should be noted that the shape of the curve was greatly influenced by yielding and strain hardening of the anchored bars. The all-sand lightweight concrete specimen test was

stopped prematurely, due to difficulties in loading the anchored bars.

General Observations on Lightweight Concrete Specimens. In general, the stress-slip curves for the all-sand lightweight and the all-lightweight specimens are quite close. If the effect of concrete strength difference is eliminated by normalizing with respect to $\sqrt{f'_c}$, the band is narrowed further and the effect of different lightweight mixes appears to be quite small. However, the 50 percent replacement mix was consistently below the other lightweight mixes.

Figure 3.11 repeats the curves presented in Fig. 3.9 and shows a curve for the 50 percent replacement lightweight with the 180° standard hook. Figure 3.11 shows that the 50 percent replacement specimens have consistently lower lead stress values for the same slip than the other two lightweight mixes studied. The 50 percent replacement specimens shown in Fig. 3.11 were cast at two different times from entirely separate concrete batches.

The 50 percent replacement specimens would have been expected to plot somewhere in the band encompassed by the all-sand lightweight specimen and the all-lightweight specimen. After careful consideration of the compressive and split tensile strengths of the different lightweight mixes, it is believed that the lower stresses observed for the 50 percent replacement mix were a direct result of these specimens having been cast using an entirely different shipment of fine as well as coarse lightweight aggregate than the one used for the other two lightweight mixes of this study. The same trend can be observed in Fig. 3.10 if the portions of the plot below lead bar stresses of 60 ksi are considered.

In summary, the effect of different lightweight concrete mixtures, insofar as the fine lightweight aggregate replacement with sand, offers very little improvement on the performance of hooked bar anchorages. It may be that some characteristic of lightweight coarse aggregates, possibly the crushing strength of the aggregate, determines the performance of the hooked bar anchorages.

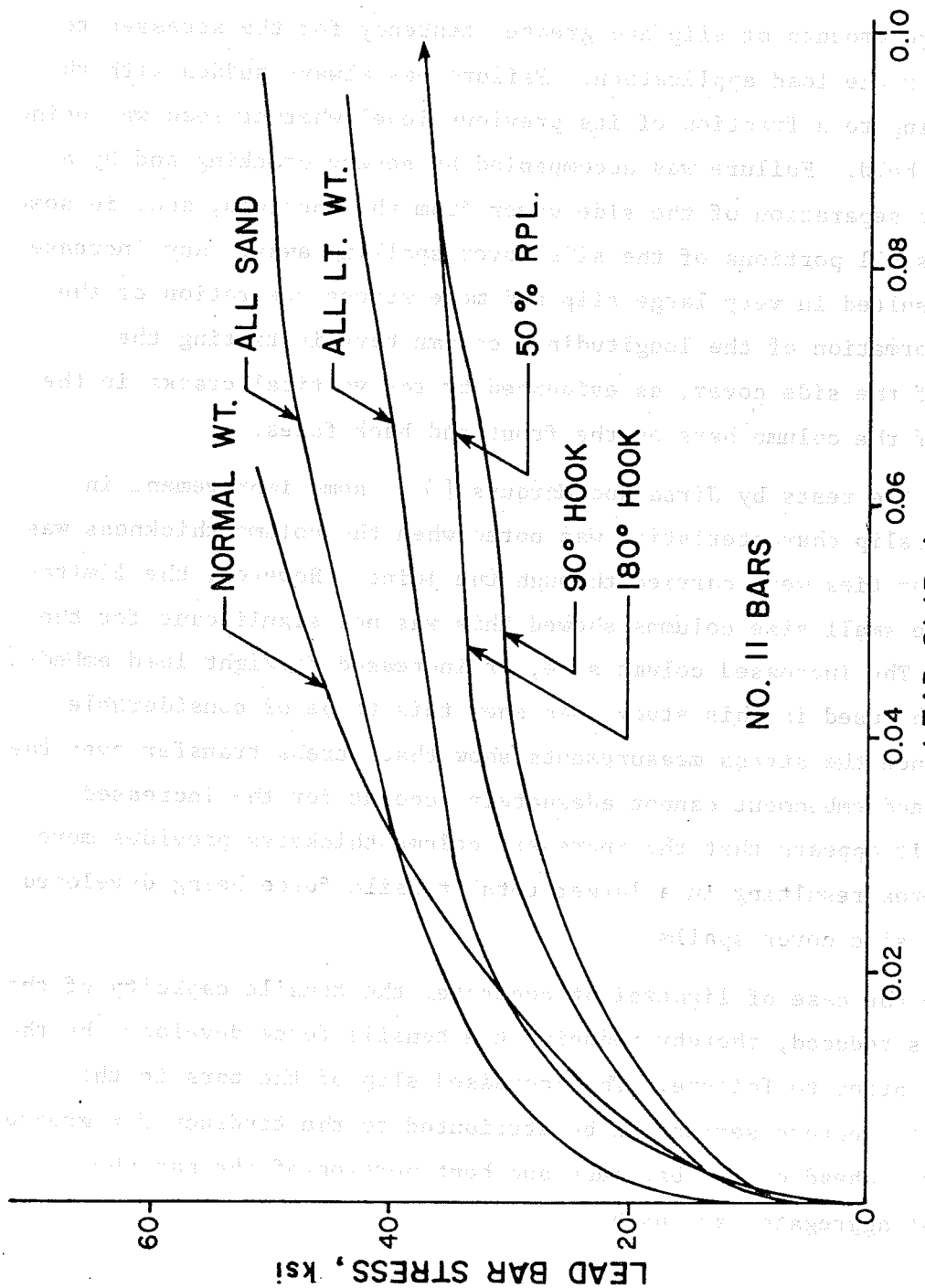

Fig. 3.11 Comparison of slip behavior of different mixes

3.3.5 Mode of Failure. All specimens followed a pattern of crack formation and failure similar to that discussed for the lead embedment series. Load increments at load stages nearing failure load showed large amounts of slip and greater tendency for the stresses to reduce after the load application. Failure was always sudden with the load dropping to a fraction of its previous level whether load was being applied or held. Failure was accompanied by severe cracking and by a significant separation of the side cover from the specimen, and, in some cases, by small portions of the side cover spalling away. Any increase of load resulted in very large slip and more severe separation of the cover, deformation of the longitudinal column bars initiating the cracking of the side cover, as evidenced by the vertical cracks in the vicinity of the column bars on the front and back faces.

In the tests by Jirsa and Marques [1], some improvement in stress and slip characteristics was noted when the column thickness was increased or ties were carried through the joint. However, the limitation to the small size columns showed this was not significant for the #11 bars. The increased column size, or increased straight lead embedment length, used in this study does show this to be of considerable value. Since the stress measurements show that stress transfer over the straight lead embedment cannot adequately account for the increased strength, it appears that the increased column thickness provides more concrete area resulting in a larger total tensile force being developed before the side cover spalls.

In the case of lightweight concrete, the tensile capacity of the concrete is reduced, thereby reducing the tensile force developed by the side cover prior to failure. The increased slip of the bars in the lightweight concrete series can be attributed to the tendency for greater deformations ahead of the bar lugs and bent portion of the bar when lightweight aggregates are used.

3.4 A Failure Hypothesis for Hooked Bars in Beam-Column Joints

Considering the measured data and observed modes of failure, a reasonable estimate of the pattern of failure of a hooked bar can be made. In nearly all cases, both in this study and in previous ones [1], the side cover spalled away at failure with a decrease in the load-carrying capacity. Therefore, it is apparent that the failure of a hooked bar is governed primarily by a loss of cover rather than pulling out. Slip between the bar and concrete produced splitting of the side cover. Starting at the lead end of the anchored bars, the splitting gradually progressed backward. As indicated by some of the stress measurements at the start of the hook, the effect of the lead slip was to reduce the stress transfer capacity along the straight lead embedment, especially for the short lengths, and this portion of the hooked bar anchorage was not transferring any stress to the concrete as failure approached.

The very large compressive stresses at the inside surface of the bend resulted in a stress condition which also tended to split the cover. As slip increased and the hook moved forward, a condition was created near failure where the hook acted similar to a wedge forcing the concrete cover to split.

3.4 Analysis of Failure Mechanisms for Tendon Force Prediction Errors

Considering the measured data not presented above in detail, reasonable explanations of the pattern of failure of a tendon can be made. In nearly all cases, even in this study and in previous ones [1], the slip zones appeared away at failure with a decrease in the load-carrying capacity. Therefore, it is apparent that the failure of a tendon is governed primarily by a loss of cover rather than pullout. Slip between the bar and concrete produced splitting at the anchorage. Strictly at the load end of the anchored bond, the splitting gradually progressed backward, as indicated by some of the strain measurements at the start of the bond, the effect of the load slip was to reduce the stress transfer capacity along the straight load embedment, especially for the short lengths, and this portion of the bonded bar anchorage was not transferring any stress to the concrete as failure approached.

The very large compressive stresses at the inside surface of the bend resulted in a stress condition which also tended to split the cover. As slip increased and the hook moved forward, a condition was brought where the hook acted similar to a wedge forcing the concrete cover to split.

4. COMPARISON OF TEST RESULTS WITH DESIGN PROCEDURES FOR HOOKED BARS

4.1 Introduction

The design provisions for hooked bar anchorages in ACI 318-71 are based primarily on provisions appearing in previous codes. Pullout tests of hooked bars embedded in massive concrete slabs provide some information, and tests on hooked bars in beam-column joints provide additional information for hooked bars with short embedment lengths. The tests performed in this study, as well as those performed earlier by Jirsa and Marques [1] and Hribar and Vasko [6] provide an opportunity to evaluate present and proposed design recommendations and to suggest changes.

In the following discussions, the strength of hooked bar anchorages will be evaluated by using the provisions of the ACI Building Code and Commentary (318-71) and the proposed design recommendations for hook strength by Jirsa and Marques [2].

4.2 Measured and Computed Strength

4.2.1 ACI Code Procedure. Using the provisions of the ACI Code Sec. 12.8, the stress developed by the standard hook is given as $f_h = \xi\sqrt{f'_c}$. Values for ξ are found in Table 12.8.1 of the ACI Code. Since a hook generally extends vertically through the concrete, it is not clear whether "top bars" or "other bars" coefficients for ξ should be used. However, for these tests, values of "other bars," where ξ is 540 for bar sizes #3 to #9, 480 for #10, and 420 for #11, resulted in hook stresses closer to the measured values.

The stress developed over the straight lead embedment, f_ℓ, was computed using the basic equation for development length, Sec. 12.5, and solving for f_ℓ in terms of a known anchorage length.

$$f_{\ell} = \frac{\ell_{\ell} \sqrt{f'_c}}{0.04A_b} \tag{4.1}$$

where ℓ_{ℓ} is the straight lead embedment and A_b is the area of the bar.

The computation of hooked bar anchorage strengths in lightweight concrete using the ACI 318-71 Code provisions is somewhat ambiguous. Different interpretations of Code provisions will yield substantially different values of predicted anchored strengths.

Section 12.5(c) of the ACI 318-71 Code specifies that "when lightweight aggregate concrete is used the basic development lengths in (a) shall be multiplied by 1.33 for all lightweight concrete and 1.18 for sand lightweight with linear interpolation when partial sand replacement is used." Section 12.8.2 of the ACI 318-71 Code specifies that "An equivalent embedment length shall be computed using the provisions of Section 12.5(a) by substituting f_h for f_y and ℓ_{ℓ} for ℓ_d." Section 12.8.2 does not specify that the provisions of Section 12.5 with all of its subsections, including Subsection 12.5(c), must be applied thereby leaving open to interpretation whether or not the standard hook strength must be modified to account for the effect of lightweight aggregate concrete or not.

If the straight lead embedment ℓ_{ℓ} is known, the stress over the straight lead embedment f_{ℓ} can be computed. The stress developed by the standard hook f_h can also be computed and the anchorage stress $(f_h + f_{\ell})$ resulting from the two interpretations of the ACI 318-71 Code procedure can be computed as indicated in Eqs. 4.2 and 4.3:

$$f = (f_h + f_{\ell}) = \frac{\xi \sqrt{f'_c}}{C} + \frac{\ell_{\ell} \sqrt{f'_c}}{0.04A_b C} \tag{4.2}$$

$$f = (f_h + f_{\ell}) = \xi \sqrt{f'_c} + \frac{\ell_{\ell} \sqrt{f'_c}}{0.04A_b C} \tag{4.3}$$

Interpretation of ACI 318-71 Code procedure based on Eq. 4.3 results in higher values of computed anchorage strengths and it was used in this study.

Using the measured concrete strengths, values of f_h (using the "other bar" coefficients), f_ℓ and computed hook strength ($f_h + f_\ell$) are tabulated in Table 4.1a. Values of computed hook strength ($f_h + f_\ell$) without usage of the lightweight concrete reduction factor are tabulated in Table 4.1b to permit direct comparisons with the normal weight concrete specimens.

It is clear from the tabulations in Table 4.1a that the ACI Code grossly underestimates the hook capacity (average $f_{hm}/f_{hc} = 1.75$, $\sigma = 0.29$) and the ultimate strength of the entire anchorage (average $f_u/(f_h + f_\ell) = 1.45$, $\sigma = 0.23$). From the values in Table 4.1b for lightweight specimens, the ACI Code provides a better estimate of hook and anchorage strength, but the ambiguity of the provisions makes it difficult to interpret the intent of the Code with respect to hooked bars in lightweight concrete.

4.2.2 Design Recommendations Proposed by Jirsa and Marques [2]. Because the ACI Code underestimated the strength of hooked bars in normal weight concrete, a different design procedure was proposed by Jirsa and Marques [2]. The strength of the hook was given as

$$f_h = 700(1 - 0.3d_b)\psi \sqrt{f'_c} \qquad (4.4)$$

where d_b is the diameter of the bar. The coefficient ψ should be taken as unity unless the following conditions are satisfied.

The value of ψ may be taken as 1.4 if (a) the bar is #11 or smaller, (b) the lead straight embedment between the standard hook and the critical section is not less than 4 bar diameters or 4 in. whichever is greater, (c) side concrete cover normal to the plane of the hooked bar is not less than 2.5 in., and (d) cover on the tail extension is not less than 2 in.

The value of ψ may be taken as 1.8 if the joint is confined by close ties at a spacing of $3d_b$ or less and meets the requirements for $\psi = 1.4$. No distinction is made between top bars and other bars.

TABLE 4.1a MEASURED AND COMPUTED ANCHORAGE STRENGTH--ACI 318-71

Normal Weight Concrete

Specimen	Measured Stresses		Computed Stresses			Meas/Comp	
	f_h	f_u	f_h Other*	f_ℓ	f_h+f_ℓ	f_{hm}/f_{hc}**	$f_u/(f_h+f_\ell)$
	ksi		ksi	ksi	ksi		
J7-90-15-1-H	66	91	36.5	26.8	63.3	1.80	1.44
J7-90-15-1-M	65	100	38.5	28.3	66.8	1.69	1.50
J7-90-15-1-L	65	97	37.8	27.6	65.4	1.72	1.48
J7-90-12-1-H	62	62	34.9	17.4	52.3	1.78	1.19
J7-90-15-2-H	73	99	37.3	27.3	64.6	1.96	1.53
J7-90-15-2-M	70	95	37.3	27.3	64.6	1.88	1.47
J7-90-15-3-H	70	104	36.8	27.0	63.8	1.90	1.63
J7-90-15-3a-H	66	98	33.1	24.3	57.4	1.99	1.71
J7-90-15-4-H	62	73	36.1	26.5	62.6	1.72	1.17
J7-180-15-1-H	64	87	34.1	24.9	59.0	1.87	1.47
J7-180-12-1-H	61	61	35.6	17.8	53.4	1.71	1.14
9-12	42	47	37.0	7.5	44.5	1.14	1.07
9-15	43	43	33.3	11.4	44.1	1.29	0.98
9-18	65	74	37.0	17.8	54.1	1.76	1.37
9-21	59	59	32.4	20.1	51.9	1.82	1.14
11-15	28	50	30.9	7.1	38.0	0.91	1.32
11-18	58	58	28.8	9.9	38.7	2.01	1.50
11-21	51	73	30.3	13.9	44.2	1.68	1.65
11-24	58	77	27.2	15.6	42.8	2.13	1.80
J11-90-15-1-H	48	48	29.0	6.6	35.6	1.66	1.35
J11-90-15-1-L	52	52	28.9	6.6	35.5	1.80	1.46
J11-90-12-1-H	42	42	28.6	3.3	31.9	1.47	1.32
J11-90-15-2-H	49	49	29.8	6.8	36.6	1.64	1.34
J11-90-15-2-L	53	53	28.2	6.4	34.6	1.88	1.53
J11-90-15-3-L	62	62	29.4	6.7	36.1	2.11	1.72
J11-90-15-3a-L	69	69	29.7	6.8	36.5	2.32	1.89
J11-180-15-1-H	45	45	27.9	6.4	34.3	1.61	1.31
					Average	1.75	1.45
					σ	0.29	0.23

*"Other bars" as defined in Sec. 12.8 of ACI 318-71 Code.

**f_{hm} - measured, f_{hc} - computed.

TABLE 4.1b MEASURED AND COMPUTED ANCHORAGE STRENGTH--ACI 318-71

Lightweight Aggregate Concrete

Specimen	ACI 318-71 f_h (Computed) "Other" ksi	ACI 318-71 f_ℓ (Computed)		$f_\ell + f_h$ (Computed Stress)		f_u Measured Stress at Failure ksi	Meas/Comp	
		with C Factor ksi	w/o C Factor ksi	with C Factor ksi	w/o C Factor ksi		with C Factor	w/o C Factor
11-90-1-L-AL	27.2	4.7	6.2	31.9	33.4	44	1.38	1.38
11-90-1-H-AL	29.1	5.0	6.7	34.1	35.8	46	1.35	1.28
11-90-1-L-AS	31.4	6.1	7.2	37.5	38.6	52	1.39	1.35
11-90-1-L-FR	28.8	5.2	6.6	34.0	35.4	38	1.12	1.07
11-180-1-L-FR	29.1	5.3	6.7	34.4	35.8	38	1.10	1.06
11-90-3-L-FR	29.7	5.4	6.8	35.1	36.5	47	1.34	1.29
7-90-1-L-AS	40.4	25.1	29.6	65.5	70.0	82	1.25	1.17
7-90-1-L-FR	36.2	21.1	26.6	57.3	62.8	80	1.40	1.27
					Average		1.29	1.23
					σ		0.11	0.14

*All values for "other bars" values for ξ

The stress developed over the straight lead embedment was computed using the ACI Code equation for development length and solving for f_ℓ in terms of a known anchorage length.

$$f_\ell = \frac{(\ell_\ell - \ell')\sqrt{f'_c}}{0.04A_b} \qquad (4.5)$$

where ℓ_ℓ is the straight lead embedment, ℓ' is $4d_b$ or 4 in. whichever is greater, and A_b is the area of the bar.

Using the measured concrete strengths, values of f_h, f_ℓ, and $f_h + f_\ell$ calculated from the recommendations proposed by Jirsa and Marques [2] are listed in Table 4.2. This approach reduces the conservatism present in the ACI Code and results in nearly the same ratios of measured to computed stress for the hook and the entire anchorage.

4.2.3 Measured Results Compared with Computed Strength. Comparing measured and computed values of f_h, the ACI Code predicts values 10 percent greater than measured for short lead embedment of #9 bars to 80 percent greater for longer embedment lengths, and 60 percent to 110 percent greater for #11 bars. The recommendations proposed by Jirsa and Marques [2] give values of f_h 10 to 50 percent greater for #9 bars and 20 to 60 percent greater for #11 bars. These results indicate that the provisions of Sec. 12.8 are quite conservative when applied to hooked bars in beam-column joints such as those tested. The Jirsa and Marques equation is in better agreement for short embedment lengths but also becomes very conservative when the embedment length is large.

The ratio of measured to computed stress at failure at the lead end of the anchorage varies from 1.0 to 1.4 for the #9 bars for both the ACI Code and the Jirsa and Marques predictions. The ratio is 1.3 to 1.8 using the ACI provisions and 1.2 to 1.6 using the Jirsa and Marques recommendations for the #11 bars. The values of lead bar stresses indicate that the stresses computed using the ACI Code for the lead straight bar length tend to be unconservative because the ratio of measured to computed lead bar stress ($f_h + f_\ell$) is less than the ratio

TABLE 4.2 MEASURED AND COMPUTED ANCHORAGE STRENGTH--JIRSA & MARQUES

Normal Weight Concrete

Specimen	Measured Stresses		Computed Stresses				
						Meas/Comp	
	f_h	f_u	f_h	f_ℓ	f_h+f_ℓ	f_{hm}/f_{hc}	$f_u(f_h+f_\ell)$
	ksi		ksi	ksi	ksi		
J7-90-15-1-H	66	91	49.0	15.5	64.5	1.35	1.41
J7-90-15-1-M	65	100	51.4	16.3	67.7	1.26	1.48
J7-90-15-1-L	65	97	50.1	15.9	66.0	1.30	1.47
J7-90-12-1-H	62	62	46.6	6.7	53.3	1.33	1.16
J7-90-15-2-H	73	99	49.8	15.8	65.6	1.47	1.51
J7-90-15-2-M	70	95	49.8	15.8	65.6	1.41	1.45
J7-90-15-3-H	70	104	49.3	15.6	64.9	1.42	1.60
J7-90-15-3a-H	66	98	56.9	14.0	70.9	1.16	1.38
J7-90-15-4-H	62	73	34.6	15.4	50.0	1.79	1.46
J7-180-15-1-H	64	87	45.7	14.5	60.2	1.40	1.44
J7-180-12-1-H	61	61	47.7	6.9	53.6	1.27	1.14
9-12	42	47	31.7	0.0	31.7	1.32	1.48
9-15	43	43	40.0	4.5	44.5	1.08	0.97
9-18	65	74	44.4	10.1	54.5	1.46	1.36
9-21	59	59	38.9	13.3	52.2	1.52	1.13
11-15	28	50	41.6	0.5	42.1	0.67	1.19
11-18	58	58	38.8	4.1	42.9	1.49	1.35
11-21	51	73	40.8	8.1	48.9	1.25	1.49
11-24	58	77	36.6	10.8	47.4	1.58	1.62
J11-90-15-1-H	48	48	39.6	0.4	40.0	1.21	1.20
J11-90-15-1-L	52	52	39.0	0.4	39.4	1.33	1.32
J11-90-12-1-H	42	42	27.4	0.0	27.4	1.53	-1.53
J11-90-15-2-H	49	49	40.0	0.4	40.4	1.23	1.21
J11-90-15-2-L	53	53	37.9	0.4	38.3	1.40	1.38
J11-90-15-3-L	62	62	39.4	0.4	39.8	1.57	1.56
J11-90-15-3a-L	69	69	51.4	0.4	51.8	1.34	1.33
J11-180-15-1-H	45	45	37.5	0.4	37.9	1.20	1.19
					Average	1.34	1.36
					σ	0.20	0.16

of measured to computed hook stress, f_h. However, in most instances the stresses computed using the proposed Jirsa and Marques Eq. 4.4 appear to be much more accurate as the two ratios are nearly equal for each test. Even though the proposed equation gives a good prediction for the increase in strength with the increase in lead embedment length, the tests show that where failure occurred prior to yielding, the stress at the start of the hook was equal or nearly equal to the stress at the lead end. Since the ACI equation for development length was based on tests in which bar stress varied from a maximum at the critical section to zero at the end of the straight bar, it seems unrealistic to use the ACI approach for computing the anchorage capacities for short bars with little stress variation along the straight portion between the critical section and the hook.

As was noted in Chapter 3, Specimens 9-15 and 9-21 were cast with a concrete of questionable quality. Observations of test results and appearance of the specimen after testing tend to indicate that poorly washed aggregate had been supplied. The crushed concrete at the inside of the hook had a tan appearance, whereas in all previous tests the crushed concrete had a whitish gray appearance. The tan coloring is likely the result of dirt and clay in the aggregate. It is possible that some of this residue built up under the hook, attributing to the large slips starting at low levels of load.

At the time of casting, the appearance of the concrete from the ready-mix truck was the same as in previous tests, giving no indication that problems would develop later. Looking at these two specimens from a serviceability point of view, it is clear that a small increase in load resulted in a large amount of slip. At stress of $0.6(f_h + f_\ell)$, a value selected to approximate service load, the slip measured was about 0.07 in. or four times the 0.016 in. suggested as permissible by the ACI Code. The use of poor quality concrete with unwashed aggregate would likely result in severe cracking at service loads.

5. PROPOSED DESIGN RECOMMENDATIONS

5.1 Introduction

Because of the observation that anchorage strength increased significantly as the lead embedment length increased, two possible approaches for the design of hooked bar anchorages will be examined. Approach A is similar to that currently in the ACI 318-71 Code and the modified version developed by Jirsa and Marques [2]. Using this approach the strength is determined by calculating a stress which can be developed by the hook plus an additional straight lead embedment to provide the difference between the hook stress and the stress at the critical section. Approach B is based on considering the hook and straight lead embedment as a unit.

To take the previously observed factors into account in developing design recommendations, the strength of hooked bar anchorages will again be divided into three classes with the distinction between these classes based on the lateral restraint provided against splitting. A modification factor ψ will be used as defined in the proposed design recommendations by Jirsa and Marques.

5.2 Approach A--Hook and Lead Embedment Considered Separately

The recommendations by Jirsa and Marques were used, as described in Chapter 4, to compute the strength of the hooks, f_h, for the specimens in this study. By deducting f_h from the strength measured at failure, f_u, the additional strength for the straight lead embedment, $f_\ell = f_u - f_h$, was determined. The results were plotted as $f_\ell/\sqrt{f'_c}$ versus ℓ_ℓ/d_b (Fig. 5.1) where ℓ_ℓ is the straight lead embedment length and d_b the bar diameter. The strength due to the lead embedment can be approximated by the

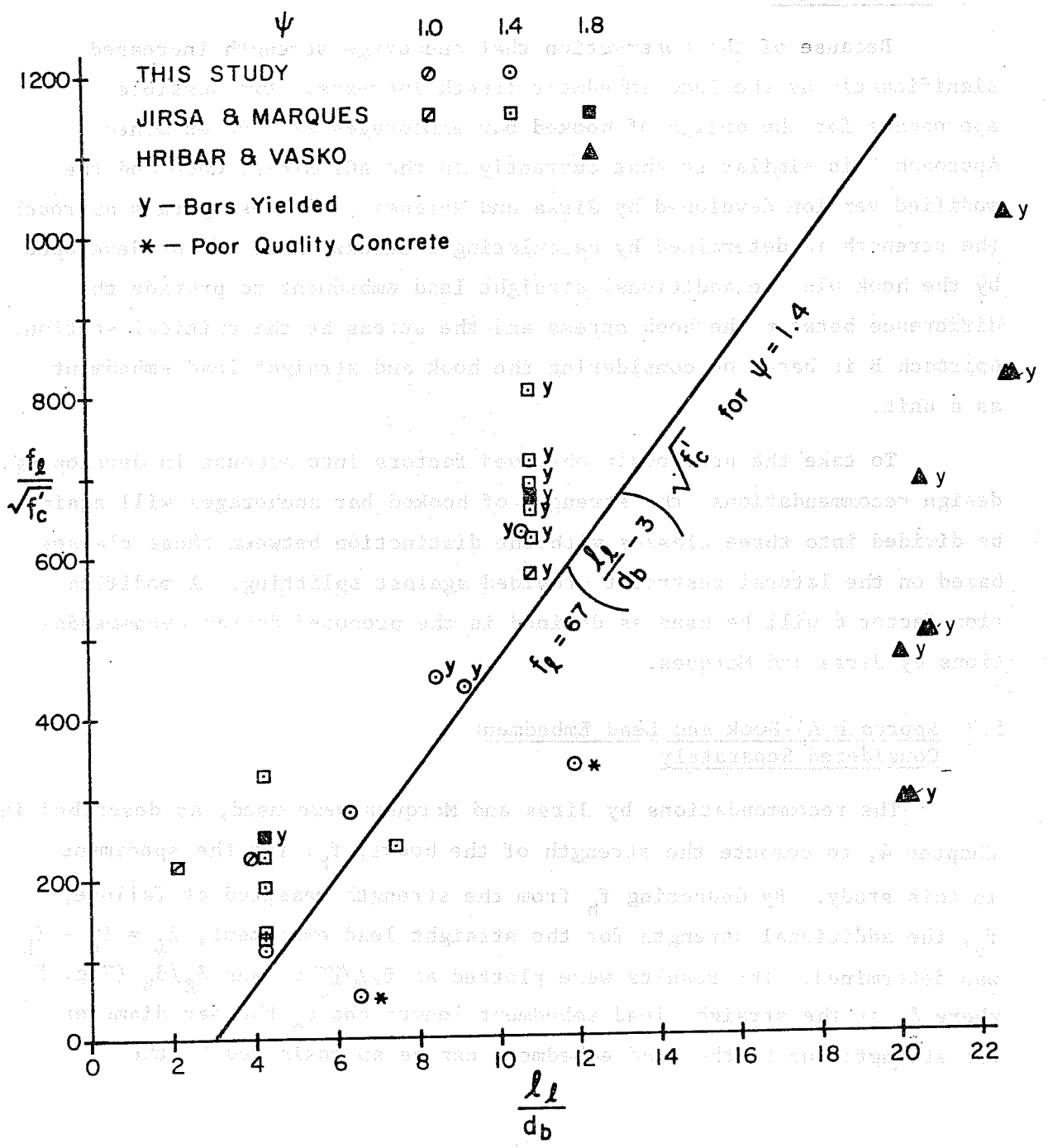

Fig. 5.1 Proposed values for strength of hooked bar anchorages using Approach A

equation

$$f_{\ell} = 67(\ell_{\ell}/d_b - 3)\sqrt{f'_c} \tag{5.1}$$

for the specimens with confinement factor $\psi = 1.4$. Reducing this equation to add the effect of confinement, and adding the equation for f_h to give the total strength of the anchored bar, f_u, results in

$$f_u = 67/1.4\ \psi(\ell_{\ell}/d_b - 3)\sqrt{f'_c} + 700\ \psi(1 - 0.3d_b)\sqrt{f'_c}$$

or, equivalently

$$f_u = 550(1 - 0.4d_b + 0.8\ \ell_{\ell}/d_b)\psi\sqrt{f'_c} \tag{5.2}$$

5.3 Approach B--Hook and Lead Embedment as a Unit

5.3.1 Length to Be Considered as Embedment Length. Two different equations can be derived, depending on how the embedment length is considered as a variable. First, the embedment length is taken as the straight lead embedment, ℓ_{ℓ}, and the strength considered is the measured strength at failure, f_u. Figure 5.2 shows $f_u/\sqrt{f'_c}$ plotted against ℓ_{ℓ}/d_b. This plot indicates that the strength for the class of specimens with $\psi = 1.4$ is given by

$$f_u = (350 + 75\ \ell_{\ell}/d_b)\sqrt{f'_c} \tag{5.3}$$

or

$$f_u = (250 + 54\ \ell_{\ell}/d_b)\psi\sqrt{f'_c} \tag{5.4}$$

Second, the embedment length is considered as the straight lead embedment plus the horizontal projected length of the hook (bend radii + d_b) and will be noted as ℓ_{dh}, Fig. 5.3.

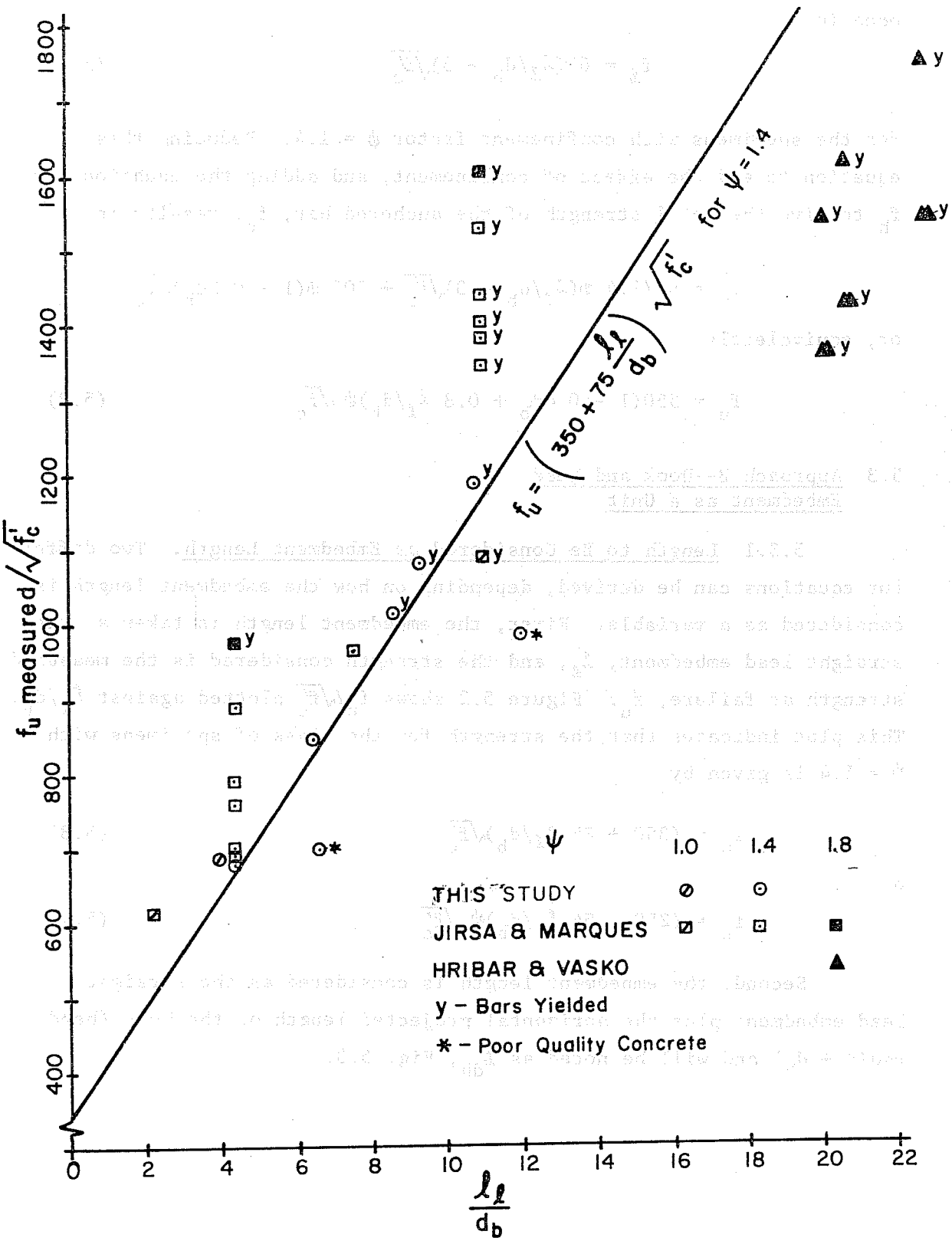

Fig. 5.2 Proposed values for strength of hooked bar anchorages using Approach B

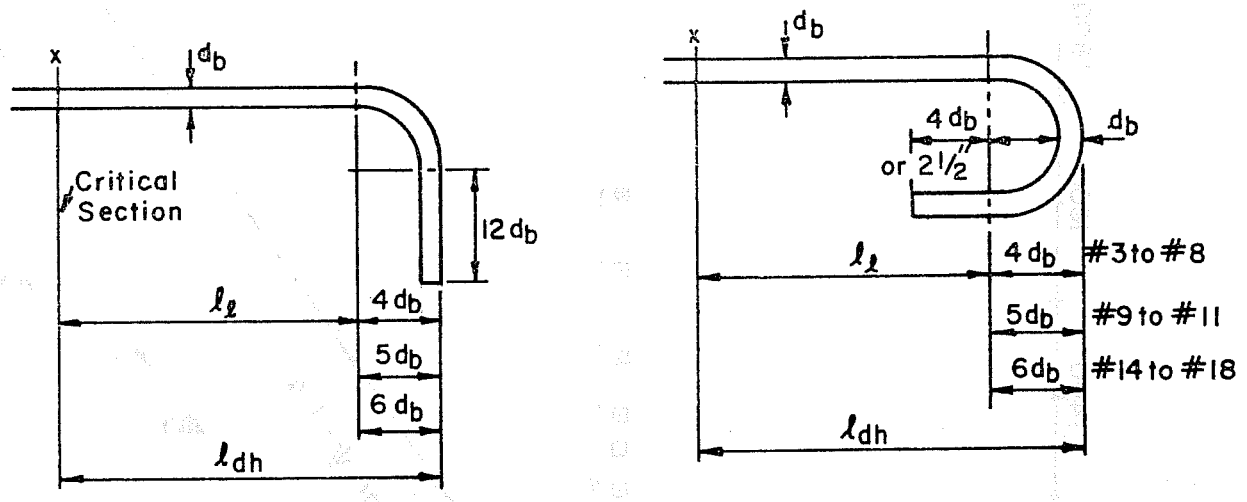

Fig. 5.3 Standard hook details

The results are plotted in Fig. 5.4 as $f_u/\sqrt{f'_c}$ versus ℓ_{dh}/d_b. A conservative line through the test results with $\psi = 1.4$ produces the following relationship

$$f_u = 70\ \ell_{dh}\sqrt{f'_c}/d_b \tag{5.5}$$

or

$$f_u = 50\ \psi\ \ell_{dh}\sqrt{f'_c}/d_b \tag{5.6}$$

5.4 Comparison of Equations

In comparing the equations from Approach A and the two equations from Approach B, the form of the equations is generally the same with the major difference being the number of terms in each equation. In each case the stress can be easily calculated as a function of the straight lead embedment length and the bar diameter. However, in practice the engineer is more often concerned with the length required to develop the yield stress of the bar rather than the stress the bar can carry for a given length. From this point of view, the equations of Approach B are much easier to use, with Eq. 5.6 being the simplest. Rearranging terms, ℓ_{dh} can be determined directly

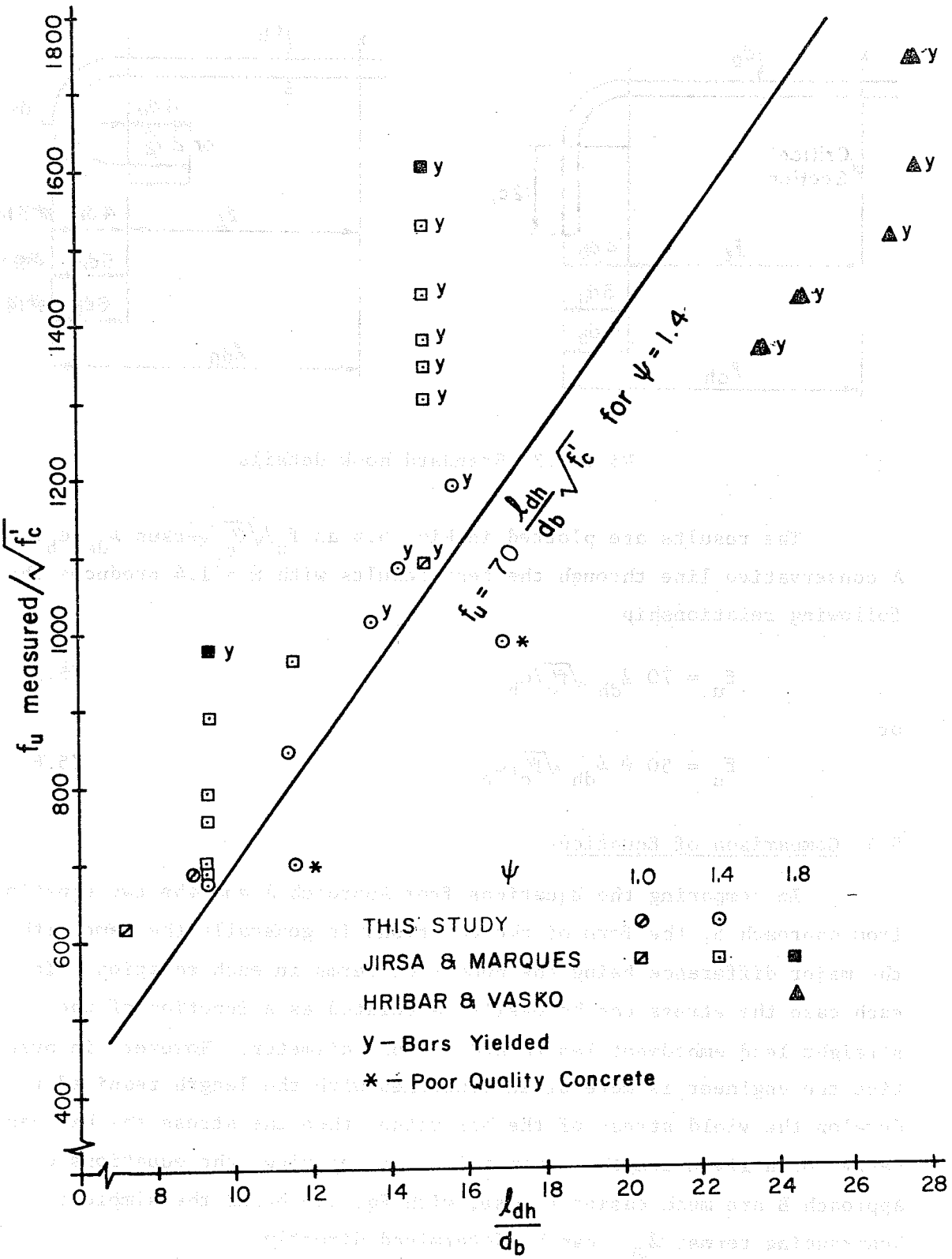

Fig. 5.4 Proposed values for strength of hooked bar anchorages using Approach B

$$\ell_{dh} = \frac{d_b}{50\psi} \frac{f_u}{\sqrt{f'_c}} \quad \text{or} \quad \frac{0.02 d_b f_y}{\psi \sqrt{f'_c}} \tag{5.7}$$

It should be noted that the length given is the total horizontal length and there is no need to add a length for the hook to determine whether the column can accommodate the hooked anchorage.

As was noted in Chapter 4, many tests showed that at failure the stress in the bar at the start of the hook was the same as that measured at the lead end of the anchorage. In all the tests, the concrete failed by splitting rather than a pullout failure of the bars. The behavior suggests that the strength is derived from the splitting strength of the concrete and it is, therefore, illogical to assume that there is a significant stress transfer along the straight length of the bar. It should be noted that for the results of tests by Hribar and Vasko in which bond release was provided over the lead embedment length, the equations of Approach B provide a better estimate of the strength than does Approach A.

Since no tests have been performed on bars of small diameter with very short lead embedment length or on bars where the hook is very near the critical section, it is difficult to determine what minimum length, if any, should be specified for the hook. The two specimens tested with ℓ_ℓ/d_b less than 4, #11 with $\ell_\ell/d_b = 2.1$ (Jirsa and Marques), and #9 with $\ell_\ell/d_b = 3.9$, give strengths well within the proposed stresses. A lower limit is obviously an embedment length, ℓ_{dh}, not less than the bend radii plus one bar diameter (the horizontal projection of the hook alone).

5.5 Design Recommendations

The following recommendations are made for determining the strength provided by hooked bars embedded in normal weight concrete.

The embedment length ℓ_{dh}, in inches, of deformed bar in tension terminating in a standard hook shall be not less than

$$\ell_{dh} = \frac{0.02 d_b f_y}{\psi \sqrt{f'_c}}$$

In no case shall ℓ_{dh} be less than $8d_b$ or 6 in., whichever is greater.

The coefficient ψ shall be taken as unity unless the following conditions are satisfied.

The value of ψ may be taken as 1.4 if (a) the bar is #11 or smaller, (b) the total embedment length, ℓ_{dh}, is not less than the minimum bend radii plus an additional embedment of five bar diameters or 4 in., whichever is greater, (c) the side concrete cover normal to the plane of the hooked bar is not less an 2.5 in., and (d) cover on the tail extension is not less than 2 in.

The value of ψ may be taken as 1.8 if the joint is confined by closed ties at a spacing of $3d_b$ or less and meets the requirements for $\psi = 1.4$.

In no case shall the embedment length, ℓ_{dh}, be less than for the standard hook.

No reduction in ℓ_{dh} shall be permitted for tail extensions or bend radii greater than required for a standard hook. For better control of deflections and cracking, 90 degree hooks are preferable.

5.6 Comparison of Proposed Recommendations with ACI and Test Results

5.6.1 Embedment Length. The proposed design recommendations are compared with ACI 318-71 provisions in Fig. 5.5, which shows the required embedment length ℓ_{dh} plotted against bar diameter.

Computed strengths using these recommendations for the bars tested in this study and by Jirsa and Marques are listed in Table 5.1. For the thirty tests available in normal weight concrete, the average ratio of measured to computed strength using Eq. 5.6 was 1.24 with a standard deviation of 0.20. Comparing these ratios with those tabulated in Table 4.1, it can be seen that the proposed equations give a better indication of strength than does the current ACI Code (average 1.45, standard deviation 0.23) and the proposal of Jirsa and Marques (average 1.36, standard deviation 0.16).

5.6.2 Slip Measurements at Working Stress Levels. In addition to the computed to measured strength ratios, Table 5.1 also lists the stress corresponding to 0.6 of the computed strength of the hooked bar

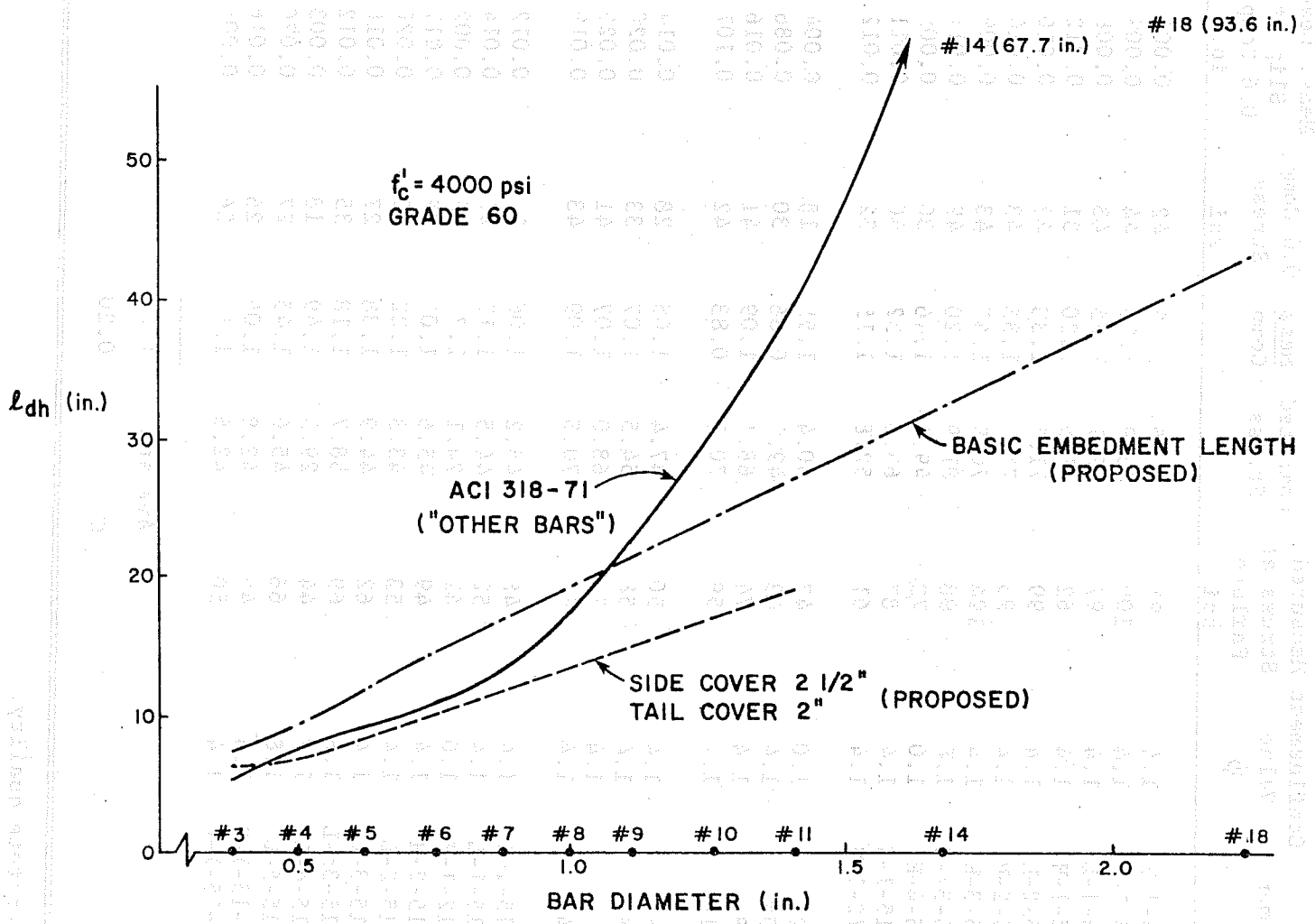

Fig. 5.5 Hook embedment length--proposed and ACI 318-71

TABLE 5.1 COMPARISON OF MEASURED AND COMPUTED ANCHORAGE STRENGTHS USING PROPOSED DESIGN RECOMMENDATIONS (NORMAL WEIGHT CONCRETE)

Specimen	Confinement Value ψ	Measured Stress at Failure ksi	Computed Stress	Meas / Comp	0.6 Comp Stress ksi	Meas. Lead Slip at 0.6 Comp. in.
J7-90-15-1-H	1.4	91	70.5	1.29	42	0.009
J7-90-15-1-M	1.4	100	73.9	1.35	44	0.009
J7-90-15-1-L	1.4	97	72.1	1.35	43	0.008
J7-90-12-1-H	1.4	62	51.5	1.20	31	0.012
J7-90-15-2-H	1.4	99	71.7	1.38	43	0.010
J7-90-15-2-M	1.4	95	71.7	1.33	43	0.014
J7-90-15-3-H	1.4	104	70.9	1.47	43	0.009
J7-90-15-3a-H	1.8	98	81.9	1.20	49	0.011
J7-90-15-4-H	1.0	73	49.8	1.46	30	0.005
J7-180-15-1-H	1.4	87	65.8	1.32	40	0.011
J7-180-12-1-H	1.4	61	52.8	1.15	32	0.012
9-12	1.0	47	30.4	1.55	18	0.004
9-15*	1.4	43	49.7	0.86	30	0.086
9-18	1.4	74	68.1	1.09	41	0.016
9-21*	1.4	59	70.7	0.83	42	0.107
11-15	1.4	50	47.4	1.05	28	0.014
11-18	1.4	58	54.5	1.07	33	0.020
11-21	1.4	73	68.0	1.07	41	0.025
11-24	1.4	77	70.8	1.09	43	0.019
J11-90-15-1-H	1.4	48	45.2	1.06	27	0.012
J11-90-15-1-L	1.4	52	44.5	1.17	27	0.014
J11-90-12-1-H	1.0	42	24.1	1.75	15	0.002
J11-90-15-2-H	1.4	49	45.6	1.07	29	0.011
J11-90-15-2-L	1.4	53	43.3	1.22	32	0.020
J11-90-15-3-L	1.4	62	44.9	1.38	27	0.016
J11-90-15-3a-L	1.8	69	58.7	1.18	35	0.012
J11-90-15-4-L	1.0	44	29.5	1.49	18	0.003
J11-90-15-5-L	1.8	66	45.6	1.45	27	0.020
J11-180-15-1-H	1.4	45	42.8	1.05	26	0.016
J11-180-15-1-L	1.4	50	42.6	1.17	26	0.005
			Average	1.24		
			σ	0.20		

*Poor concrete quality.

anchorage and the lead slip measured at a stress level of 0.6 of the computed strength. The reason for these comparisons is to give an indication of the possible crack width at the beam-column joint due to slip of the anchorage at service loads. The limit for crack width suggested in the ACI Code Commentary (Sec. 10.6) is 0.016 in. The figures indicate that, except for Specimens 9-15 and 9-21, only five specimens had a slip greater than 0.016 in. at the assumed service load stress, with the largest slip being 0.025 in. In each case, a #11 bar was tested with a low level of axial load (700 to 800 psi) applied to the columns, and in two cases the computed stress is greater than the yield stress of the bars tested.

In evaluating the proposed design recommendations, those recommended by Jirsa and Marques, and those contained in ACI 318-71, it is evident that the main gap in the experimental results is the lack of data for bars with the start of hook located at the critical section and bars with a minimum amount of cover. In addition, data are needed to determine the confinement characteristics of bars embedded im "mass concrete." Based on the current data available, it appears that design procedures can be adjusted to reflect realistically the strength of hooked bar anchorages considering the hook and the straight lead embedment as a unit.

5.7 Modification of Design Recommendations for Lightweight Concrete

Table 5.2 lists the lead bar stress at failure (f_u) for the eight lightweight specimens and the computed strength using Eq. 5.6. Ratios of measured to computed bar stresses at failure are tabulated. No reduction was applied to computed strengths to account for the effect of lightweight concrete. The ratios of measured to computed stresses at failure varied from 0.85 to 1.07 for #11 bars and from 1.05 to 1.15 for #7 bars.

TABLE 5.2 MEASURED AND COMPUTED ANCHORAGE STRENGTHS (LIGHTWEIGHT AGGREGATE CONCRETE)

Specimen	Confinement ψ	f_u Measured Stress at Failure (ksi)	Computed (ksi) Eq. 5.6	Meas / Comp Eq. 5.6	Computed (ksi) Eq. 5.8	Meas / Comp Eq. 5.8	0.6 Computed Stress (ksi)	Meas. Lead Slip at 0.6 Comp. Stress (in.)
11-90-1-L-AL	1.4	44	42.0	1.05	34.9	1.26	21	0.007
11-90-1-H-AL	1.4	46	44.9	1.02	37.3	1.23	22	0.009
11-90-1-L-AS	1.4	52	48.5	1.07	40.3	1.29	24	0.004
11-90-1-L-FR	1.4	38	44.4	0.86	36.9	1.03	22	0.017
11-180-1-L-FR	1.4	38	44.9	0.85	37.3	1.02	22	0.014
11-90-3-L-FR	1.4	47	45.8	1.03	38.0	1.24	23	0.018
7-90-1-L-AS	1.4	82	77.8	1.05	64.6	1.27	39	0.007
7-90-1-L-FR	1.4	80	69.8	1.15	57.9	1.38	35	0.005
			Average	1.01		1.22		
			σ	0.10		0.13		

Because the average ratio of measured to computed strength is lower for the lightweight specimens (1.01) as compared with the normal weight specimens (1.24 from Table 5.1), an adjustment for lightweight concrete is needed to make the ratios for both materials coincide more closely. It should be noted that there is no tendency for all-lightweight specimens (AL) to give lower values than those with all fines replaced by sand (AS). Because the number of tests was small, it was decided to propose one factor covering all mixes with lightweight aggregate. As discussed previously, it appears that the behavior may be significantly determined by the characteristics of the coarse lightweight aggregate.

Using this approach, the adjustment factor Ω for lightweight concrete was calculated as $\Omega = 1.01/1.24 = 0.82$. Because the equation for ℓ_{dh} involves the inverse of Ω, the term was changed to 0.83 which results in a 20 percent adjustment for lightweight concrete.

The design recommendation proposed previously, Eq. 5.6, is modified by the coefficient Ω to produce the following equation:

$$f_u = 50\psi \Omega \ell_{dh}\sqrt{f'_c}/d_b \qquad (5.8)$$

where $\Omega = 0.83$ and ψ is as defined in Chapter 4.

Table 5.2 shows computed anchorage strengths using the modified design recommendations (Eq. 5.8) and the ratios of measured to computed strength. The ratios of measured to computed stresses obtained using the proposed design recommendations vary from 1.02 to 1.38, with an average ratio of measured to computed strength of 1.22, and with a standard deviation of 0.13. The measured lead slip at a value of lead bar stress equal to 0.6 of the computed anchorage strength is also given, and as can be seen all specimens are below or very near the suggested limit for crack width of 0.016 in.

With the modification for lightweight concrete, the proposed method for predicting the hooked bar anchorage strengths requires the use of one equation to obtain the required strength and embedment

length, whereas the ACI 318-71 Code procedure requires the use of a table to obtain the stress developed by the hook while the remainder of the stress required by the anchorage must be supplied by a straight lead embedment. The lead embedment is obtained by means of a second equation that must be adjusted to reflect the type of lightweight aggregate concrete used. The simplicity of application of the proposed method is obvious. In addition, ambiguity regarding lightweight concrete is eliminated.

6. SUMMARY AND CONCLUSIONS

6.1 Test Program

In order to investigate the influence of straight lead embedment and lightweight concrete on the strength of hooked bar anchorages, sixteen specimens were tested. These specimens and the method of testing were patterned after a previous study of hooked bar anchorages so that direct comparisons could be made. The lead embedment length varied with the depth of the column in which the bar was embedded. The bars were loaded in tension to failure to establish basic strength and stiffness characteristics. The slip of the anchored bars with respect to the concrete and stress transferred to the concrete along the bars were measured.

The results of the test program and the results of previous tests were combined to develop a relatively simple relationship between the embedded length of a hooked bar and strength. Using the relationship developed for strength, the performance of the anchored bars appears to be within acceptable limits of serviceability as set by the ACI 318-71 Code.

6.2 Conclusions

Based on the evaluation and discussion of test results from this and previous studies of hooked bar anchorages, the following conclusions can be made:

(1) A failure hypothesis was developed which appears to explain the basic behavior of hooked bar anchorage. The failure of a hooked bar is governed primarily by a loss of cover rather than by pulling out. Stress measurements indicate that at failure of the concrete very little, if any, stress is

transferred to the concrete along the straight lead embedment for small ratios of lead embedment to bar diameter.

(2) The principal factors affecting anchorage capacity are the length of embedment and the degree of lateral confinement of the joint.

(3) Replacement of lightweight aggregate fines with sand fines does not seem to significantly affect the strength of hooked bars anchored in lightweight aggregate concrete based on the eight tests reported. More studies are required to confirm this finding. A characteristic of lightweight aggregate, possibly the crushing strength of the coarse aggregate, seems to be of major importance insofar as the strength of hooked bar anchorages is concerned.

(4) The equation

$$f_u = 50 \frac{\ell_{dh}}{d_b} \Omega \psi \sqrt{f'_c}$$

can be used to adequately predict the strength developed by a hooked bar. This equation reflects the principal factors affecting anchorage capacity and the fact that the straight lead embedment and the hook act together as a unit to develop the strength.

(5) Research is needed to examine the significance of lateral reinforcement in relation to the straight lead embedment. Research is also needed to establish the strength of hooked bars with short embedment lengths in mass concrete. Data are also needed for bars of small diameter with hooks located near the critical section and for groups of closely spaced bars. The results of the limited study reported herein only provide an indication of the anchorage strength for a high degree of confinement.

6.3 Design Recommendations--Model Code Clause for Standard Hooks

6.3.1 The embedment length ℓ_{dh}, in inches, of deformed bars in tension terminating in a standard hook shall be computed as the product of the basic embedment length from Sec. 6.3.2 and the applicable factor or factors in Sec. 6.3.3, but ℓ_{dh} shall not be less than $8d_b$ or 6 in., whichever is greater.

6.3.2 The basic embedment length shall be computed by:

$$\ell_{dh} = \frac{0.02\ d_b f_y}{\sqrt{f'_c}}$$

6.3.3 The basic embedment length shall be multiplied by the applicable factor or factors for:

6.3.3.1 #11 bars or smaller with side cover normal to the plane of the hooked bar not less than 2-1/2 in. and cover on the tail extension of not less than 2 in. 0.7

6.3.3.2 #11 hooked bars or smaller with side cover of not less than 2-1/2 in., tail extension cover of not less than 2 in., and enclosure by closed stirrups or hoops at a spacing of $3d_b$ or less. 0.55

6.3.3.3 Lightweight aggregate replacing all or a portion of the aggregate. 1.20

6.3.4 Hooks shall not be considered effective in compression.

6.3 Heating Requirements for Residential Areas
(Climate Zone Discovery Method)

6.3.1 The underdrawn temp T_{dp} in Celsius, of air measured here is required by to a reference here shall be measured on the product as the Sec. 6.3.2 and the applicable temperature in Sec. 6.3.3, the T_{dp} shall not be less than $T_{dp} = T_{dp}$, whichever is greater.

6.3.2 The basic underdrawn temp shall be determined by

$$T_{dp} = \frac{0.0 \cdot T_{dp}^2}{\sum}$$

6.3.3 The basic underdrawn temp shall be multiplied by the applicable factor or factors here:

6.3.3.1 All here or needles with this cover mounted on the plane of the hooked pan not less than 2-1/2 in. the cover to the pad extended no not less than 2 in.

6.3.3.2 All hooked here or needles with this cover of not less than 2-1/2 in., pad-separation cover of less than 2 in., and enclosure by closed stirrups or here no a spacing of S_{dp} or less.

6.3.3.3 Hydrodynamic aggregate including all or a portion of the aggregate.

6.3.3 Means shall not be considered effective in determining

REFERENCES

1. Jirsa, James O., and Marques, Jose L. G., A Study of Hooked Bar Anchorages in Beam-Column Joints, Final Report to Reinforced Concrete Research Council, Project 33, Austin, 1972.

2. Marques, Jose L. G., and Jirsa, James O., "A Study of Hooked Bar Anchorages in Beam-Column Joints," Journal of the American Concrete Institute, Proc. V. 72, No. 5, May 1975, pp. 198-209.

3. Minor, John, and Jirsa, James O., "Behavior of Bent-Bar Anchorages," Journal of the American Concrete Institute, Proc. V. 72, No. 4, April 1975, pp. 141-149.

4. ACI Committee 318, Building Code Requirements for Reinforced Concrete (ACI 318-71), American Concrete Institute, Detroit, 1971.

5. ACI Committee 318, Commentary on Building Code Requirements for Reinforced Concrete (ACI 318-71), American Concrete Institute, Detroit, 1971.

6. Hribar, J. A., and Vasko, R. C., "End Anchorage of High Strength Steel Reinforcing Bars," Journal of the American Concrete Institute, Proc. V. 66, No. 11, November 1969, pp. 875-883.

7. Pinc, Robert L., "The Influence of Lead Embedment on the Strength of Hooked Bar Anchorages," MS thesis, The University of Texas at Austin, May 1976.

8. Watkins, Michael D., "The Influence of Lightweight Aggregate Concrete on the Strength of Hooked Bar Anchorages," MS thesis, The University of Texas at Austin, May 1977.

1. Jirsa, James O., and Breen, John E., "A Study of Bonded Reinforcement in Beam-Column Joints," Final Report to Getty/Exxon Concrete Research (Austin, Texas), Jan. 1979.

2. Meinheit, Donald F., and Jirsa, James O., "A Study of Bonded Reinforcement in Beam-Column Joints," Journal of the Structural Division, ASCE, Vol. 107, No. ST5, May 1981, pp. 975-991.

3. Meinheit, Donald F., and Jirsa, James O., "Shear Strength of Reinforced Concrete Beam-Column Joints," Journal of the American Concrete Institute, Vol. 74, No. 4, April 1977, pp. 169-172.

4. ACI Committee 318, Building Code Requirements for Reinforced Concrete (ACI 318-71), American Concrete Institute, Detroit, 1971.

5. ACI Committee 318, Commentary on Building Code Requirements for Reinforced Concrete (ACI 318-71), American Concrete Institute, Detroit, 1971.

6. Bresler, B. A., and Wasko, R. D., "Bond Anchorage of High Strength Steel Reinforcing Bars," Journal of the American Concrete Institute, Proc. V. 60, No. 11, November 1963, pp. 877-886.

7. Pina, Rolando L., "The Influence of Lead Debonding on the Strength of Hooked Bar Anchorages," MS Thesis, The University of Texas at Austin, May 1979.

8. Meinheit, Michael D., "The Behavior of Reinforcing Anchorages in the Tension Zone of Hooked Bar Anchorages," MS Thesis, The University of Texas at Austin, May 1977.